

# ANALYSIS OF TORSIONAL VIBRATIONS IN ROTATING MACHINERY

by

**J. C. (Buddy) Wachel**

President

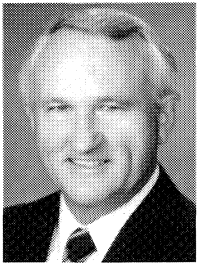
and

**Fred R. Szenasi**

Senior Project Engineer

Engineering Dynamics Incorporated

San Antonio, Texas



*J.C. (Buddy) Wachel is President of Engineering Dynamics Incorporated, an independent consulting firm. He has over 35 years of experience and has published over 30 technical papers. He has solved problems worldwide in piping vibrations, lateral and torsional critical speeds, rotor instabilities, and crankshaft failures. In addition to the practical field experience, he supervises the computer design audits of machinery and piping to ensure that the systems will have*

*acceptable vibrations and stresses. He has BSME and MSME degrees from the University of Texas. He is an ASME Fellow, a member of the Vibration Institute, and is a registered Professional Engineer in Texas.*



*Fred R. Szenasi is a Senior Project Engineer at Engineering Dynamics Incorporated. He has specialized in assessing the reliability of industrial machinery for 27 years. His expertise in rotordynamics includes the analysis of rotor instabilities, balancing turbines and compressors, prediction of vibrational displacement, stress, and methods of failure detection. He has developed computer programs for solving rotordynamics problems including torsional*

*and lateral critical speeds, rotor response, and instabilities. He has a B.S.M.E. degree from Texas Tech University and an M.S.M.E. degree from the University of Colorado. He is a registered Professional Engineer in the State of Texas, and a member of ASME and the Vibration Institute.*

reliability of a rotary equipment train. Accurate response prediction requires analysis techniques which consider all forcing functions in the system in addition to the mass-elastic properties of the shafts, couplings, gears, impellers, etc.

The severity of the torsional oscillations and stresses depends upon the relationship between the operating speed and excitation frequencies of unsteady torques and the torsional natural frequencies and mode shapes of the shaft system (critical speeds). The difference between these frequencies is referred to as the separation margin. The magnitude of the stress also depends upon the amplification factor on resonance (damping) and the stress concentration factors.

The API Codes for Turbines, Compressors, and Pumps (611, 617, 610) specify that the torsional modes of the complete unit should be at least 10 percent below any operating speed or at least 10 percent above the trip speed. In some systems, multiples of operating speed and blade passing frequencies can excite torsional natural frequencies. These potential problems should be addressed in purchase specifications to avoid conflicts. An additional margin of at least five percent should be allowed for calculation inaccuracy in torsional analyses. Variable frequency drive motors typically operate from 20 percent to 100 percent of the motor design speed, making it virtually impossible to meet the API specification. Other types of drivers with wide speed ranges may have similar problems. In these cases where detuning is not practical, more detail analyses with particular emphasis on accurate stress prediction is essential to determine reliability.

## ANALYSIS REQUIREMENTS

After the equipment design is finalized, torsional analyses should be performed to demonstrate that the system has a high degree of reliability. Harris and Crede [1], Nestorides [2], Wilson [3], and Rotordynamics of Machinery [4], provide references on torsional analysis procedures. The depth of the analysis necessary to assess the reliability of a torsional system depends upon the frequencies of the exciting energy and the location of the torsional natural frequencies.

An acceptable torsional system is generally one that avoids any coincidence of an operating speed or torsional excitation harmonic with a torsional natural frequency. Therefore, the torsional natural frequencies of the system should be calculated and the excitation forces that will exist in the system have to be defined. It is convenient to develop an interference diagram which identifies possible coincidences between the expected excitation frequencies and the calculated torsional natural frequencies within the operating speed range. Examples for typical systems are given in Table 1 and Figures 1 and 2. Each upward sloping line on the interference diagram represents a single mechanical or electrical excitation frequency or harmonic; when they cross a torsional natural frequency (horizontal line), a torsional resonance would

## INTRODUCTION

All rotating machinery systems experience torsional oscillations to some degree during startup, shutdown, and continuous operation. Consequently, the torsional response characteristics of rotating and reciprocating equipment should be analyzed and evaluated to ensure the system's reliability. Severe torsional vibrations often occur with the only indication of a problem being gear noise or coupling wear. Excessive torsional vibrations can result in gear wear, gear tooth failures, key failures, shrink fit slippage, and broken shafts in severe cases.

The torsional vibration response of rotating machinery components is an important consideration in defining the operational

Table 1. Mass/Elastic Data of 800 HP Motor System.

| MASS NO. | DIAM. inches | WR2 in-lb-s <sup>2</sup> | K (1E-6) in-lb/rad | STATION DESCRIPTION |
|----------|--------------|--------------------------|--------------------|---------------------|
| 1        | 7.75         | 49.43                    | 712.00             | MOTOR               |
| 2        | 7.75         | 92.58                    | 712.00             | MOTOR               |
| 3        | 7.75         | 92.58                    | 712.00             | MOTOR               |
| 4        | 7.75         | 92.58                    | 712.00             | MOTOR               |
| 5        | 7.75         | 92.58                    | 712.00             | MOTOR               |
| 6        | 7.75         | 92.58                    | 712.00             | MOTOR               |
| 7        | 7.75         | 92.58                    | 712.00             | MOTOR               |
| 8        | 7.75         | 92.58                    | 712.00             | MOTOR               |
| 9        | 4.00         | 47.11                    | 32.36              | MOTOR               |
| 10       | 1.72         | 40.64                    | 8.96               | CPLG                |
| 11       | 6.00         | 13.43                    | 110.32             | PUMP                |
| 12       | 6.75         | 11.60                    | 174.94             | PUMP                |
| 13       | 0.00         | 907.94                   | 0.00               | IMPELLER            |

occur. The solid circle identifies the possible torsional resonant condition. For some systems, an interference diagram may be all that is needed to show that the torsional resonances will not be excited.

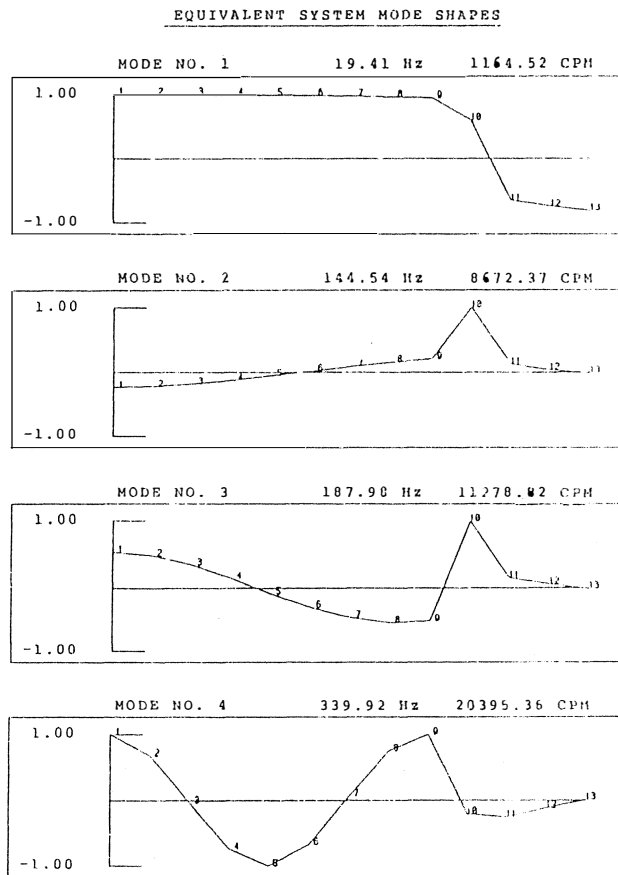


Figure 1. Torsional Natural Frequencies and Mode Shapes.

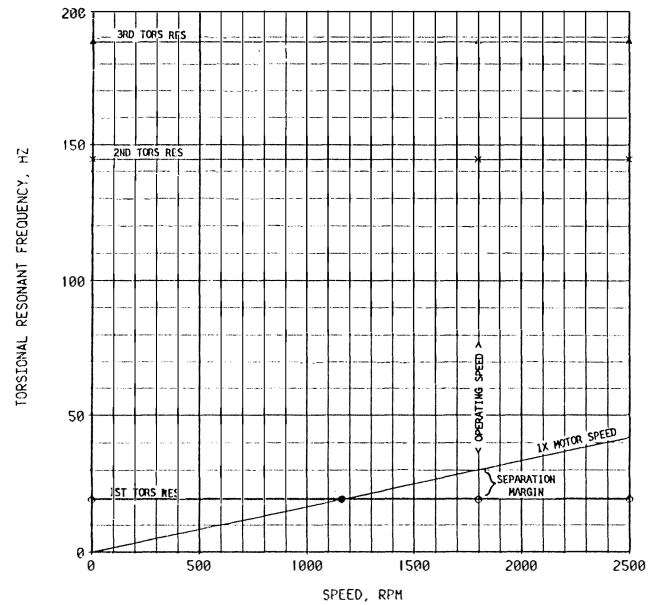


Figure 2. Interference Diagram—Single Speed—Single Exciting Order.

If torsionally resonant conditions cannot be avoided, then a detailed stress analysis should be performed to determine if the resulting stresses are below the endurance limit stress for the shaft material. A detailed steady-state torsional analysis would include:

- Calculation of the torsional natural frequencies.
- Calculation of the torsional mode shapes.
- Development of the interference diagram.
- Definition of the coincidence of the excitation frequencies with the torsional natural frequencies.
- Calculation of the dynamic torsional oscillations at all the masses in the system, based on the expected dynamic torque modulations, stress concentration factors, and amplification factors.
- Calculation of the dynamic torsional stresses in all the shafts, based on the expected dynamic torque modulations, stress concentration factors, and amplification factors.
- Comparison of the calculated results with applicable codes or specifications to determine compliance with regard to separation margin, stresses, gear loading, and coupling dynamic torque.
- Parametric analysis to determine possible coupling modifications when the separation margin, stress levels, and coupling torque are not acceptable.

A full torsional analysis may not be necessary for some simple systems. The degree of detail necessary to identify any potential problems depends on the system and its operating conditions. Consider the following examples which represent systems of various degrees of complexity.

*Single Speed—Single Exciting Order*

For a constant speed system, it may be sufficient to calculate the torsional natural frequencies of the system and determine the separation margin. An interference diagram for the system will indicate the separation margin as shown in Figure 2. If there is a 20 percent separation margin between the operating speed and any torsional natural frequency, then the system generally can be considered acceptable. Coupling stiffness changes can be considered to move the torsional natural frequency, if necessary.

*Single Speed—Multiple Exciting Harmonics*

Multiple exciting harmonics increase the chance for a coincidence of a speed or one of its harmonics with a torsional natural frequency (Figure 3). This example represents a motor driving a centrifugal pump with a gear ratio of 2 to 1. Possible dynamic torque excitation from the gear, the pinion, and the pump impeller blade passing frequency (five blades) is considered. Other examples would be systems with reciprocating equipment, or a centrifugal compressor with energy at its blade passing frequency. In reciprocating equipment, several of the multiples of running speed may be major orders with significant energy. The major orders must be identified and separated from the torsional natural frequencies. In high speed rotating equipment, such as centrifugal compressors, turbines, and motors, the higher harmonics typically have less energy than the fundamental.

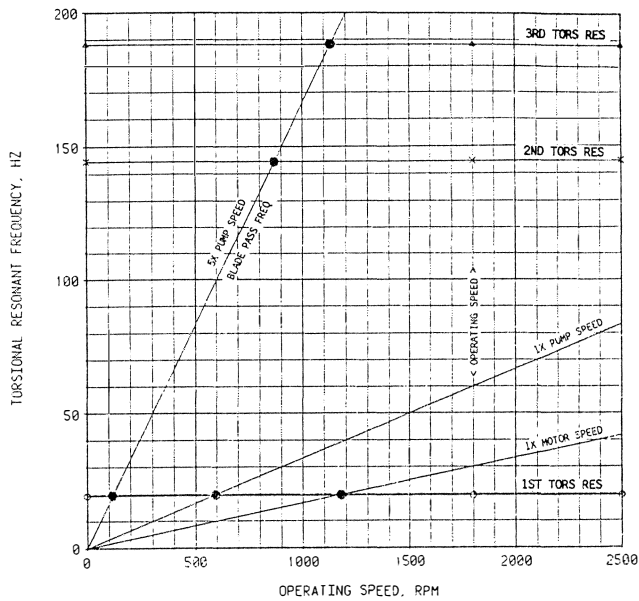


Figure 3. Interference Diagram—Single Speed-Multiple Exciting Orders.

If a sufficient separation margin cannot be maintained between the torsional natural frequencies and all the exciting orders, then a forced response analysis should be performed to calculate the torsional amplitudes and stresses. Shaft stresses should be less than the endurance limit stress for unlimited life.

*Multiple Speeds—Multiple Exciting Orders*

A system with a wide operating speed range and multiple exciting orders makes it virtually impossible to avoid all coincidences with the torsional natural frequencies (Figure 4). Examples are systems which have reciprocating engines or compressors or systems driven by variable frequency drive motors. These systems require additional considerations in the design stage over conventional constant speed equipment. The wide speed range increases the likelihood that, at some operating speed, a coincidence between a torsional natural frequency and an harmonic excitation frequency will exist.

For systems with reciprocating compressors and engines, a torque-effort curve needs to be developed from the cylinder pressures and phase data. The unsteady torque will have many frequency components (harmonics) which must be included to calculate a realistic forced response. Compressors and two-cycle

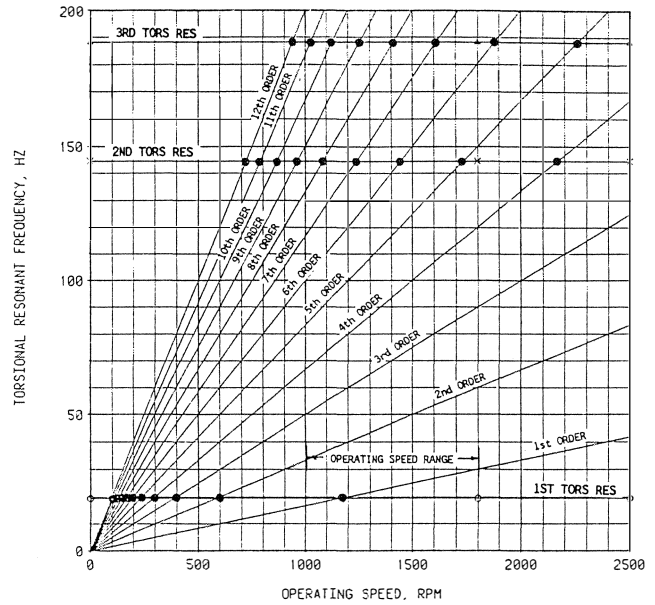


Figure 4. Interference Diagram—Multiple Speeds-Multiple Exciting Orders.

engines will have integer orders, but four-cycle engines will also have half-frequency orders corresponding to the firing frequency.

In variable frequency drive (VFD) motors, lower orders at 1x, 6x and 12x of electrical energy are created which may have significant dynamic torques. A full analysis is usually required to calculate the shaft stresses and coupling torques, and to compare them to applicable criteria. Constant speed motor systems which are converted to VFD operation can have a greater potential for torsional resonances because of the wider speed range and additional harmonics (compare Figure 2 with Figure 4).

*Transient Conditions*

Optional analyses for motors and generators may be required for transient operating conditions including:

- Calculation of the dynamic torques and transient stresses imposed on the system during startup.
- Calculation of the dynamic torques and stresses for an electrical fault.
- Evaluation of the fatigue life or number of acceptable startups for the transient startup, based on cumulative fatigue theory.

*Startup*

A system which passes through a torsional natural frequency during startup may produce significant transient shaft stresses. If the system is started on a frequent basis, a startup analysis should be performed to determine if low cycle fatigue is a potential problem. Synchronous motors definitely need a transient torsional startup analysis.

During startup, when a system accelerates through a resonance, the stresses will normally be lower than the calculated steady-state values. Therefore, the calculated steady-state values can be compensated for acceleration during startup, system damping, and the resonant frequency, in order to determine if damage will be done. An apparent lower amplification factor results from rapid acceleration through resonance as shown in Figure 5, which includes the effects of the natural frequency,  $F_n$ , and acceleration rate, (a). These startup stresses can be accurately calculated by performing

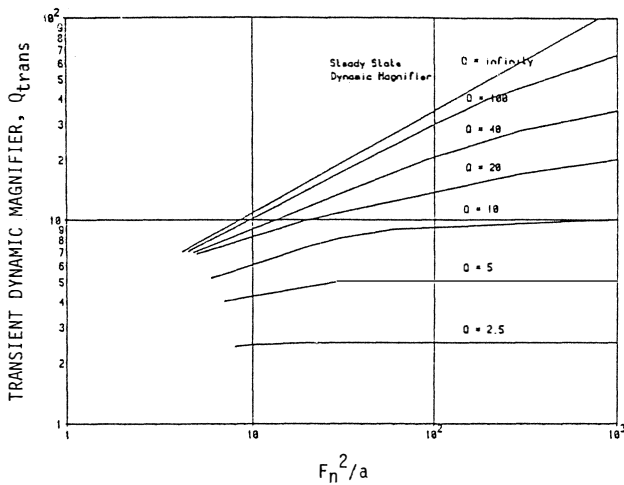


Figure 5. Reduction in Dynamic Modifier Due to Acceleration through Resonance.

a time-domain transient analysis; however, this is normally not needed to assess the reliability of the system, since a simplified analysis should show those systems that may have problems.

Electrical Faults

Motors and generators which may be subjected to an electrical fault should be analyzed to calculate the peak shaft stress and coupling torque. Comparison with the shaft yield stress in shear and the maximum allowable peak torque of the coupling will determine if the system can withstand the fault without damage. Although the coupling is usually chosen on the basis of mean torque requirements for the full load condition, it must also have a sufficient service factor to handle any likely overloads.

Problem Solving

If the torsional analyses identify problems in the system, a parametric analysis can identify sensitive elements (those stiffness or mass components that most influence the natural frequencies and responses) that may be adjusted to modify the torsional responses and make the system acceptable. If problems are detected, those items most influential could be adjusted in an attempt to reduce the torsional amplitudes:

- *System torsional frequencies*—possible changes: coupling stiffness, shaft stiffness (diameter), change in the mass inertia (material, size), or addition of a flywheel.
- *System damping*—possible changes: add a coupling with elastomeric elements or a viscous damper.
- *Torque excitation*—possible changes: reduce amplitudes (alternate driver); change speeds (different gear ratio, or operating speed); change engine firing order.
- *Stress concentration factors*—improve geometry at stress risers.

If the critical speeds cannot be removed from the desired operating speed range, they should be avoided by a 10 percent margin, if feasible. For example, if the operating speed coincides with a critical speed at Z, then the system should avoid speeds between 0.9 Z and 1.1 Z.

If avoidance is not possible, a detailed stress analysis should be performed to determine if the stresses are below the endurance limit stress for the shaft material.

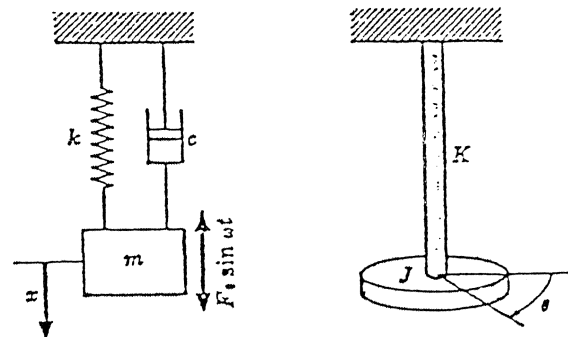
THEORY

The theory of torsional vibration is simple and the solution for the torsional natural frequencies of a shafting system is straightforward. The torsional oscillation of a cylindrical shaft is based upon the following formula:

$$\theta(t) = T(t) \frac{L}{I_p G} \tag{1}$$

This equation indicates that angular time oscillations  $\theta(t)$  of a shaft are based upon a time-varying torque  $T(t)$  and the elastic parameters of the shaft (length, L; polar moment of inertia,  $I_p$ ; material shear modulus, G). The above equation is for a simple uniform beam (Figure 6) fixed on one end with a predictable time-varying torque on the other free end. A comparison of the single degree-of-freedom equation for torsional and rectilinear systems are compared in Table 2.

Table 2. Nomenclature for Rectilinear and Torsional Vibrations.



Equivalent Single-Degree-of-Freedom Models

|                        | Rectilinear vibration   |                         | Torsional vibration   |                             |
|------------------------|---|-------------------------|---|-----------------------------|
|                        | Symbol  | Unit                    | Symbol  | Unit                        |
| Time                   | t   | sec                     | t   | sec                         |
| Displacement           | z   | in                      | $\theta$  | rad                         |
| Velocity               | $\dot{z}$   | in/sec                  | $\dot{\theta}$  | rad/sec                     |
| Acceleration           | $\ddot{z}$  | in/sec <sup>2</sup>     | $\ddot{\theta}$   | rad/sec <sup>2</sup>        |
| Spring constant        | k   | lb/in                   | K   | in-lb/rad                   |
| Damping coefficient    | c   | lb-sec/in               | $\gamma$  | in-lb-sec/rad               |
| Damping factor         | f   | dimensionless           | $\zeta$   | dimensionless               |
| Mass                   | m   | lb-sec <sup>2</sup> /in | J   | lb-in-sec <sup>2</sup> /rad |
| Force or torque        | $F = m\ddot{z}$   | lb                      | $T = J\ddot{\theta}$  | in-lb                       |
| Momentum               | $m\dot{z}$  | lb-sec                  | $J\dot{\theta}$   | in-lb-sec                   |
| Impulse                | Ft  | lb-sec                  | Tt  | in-lb-sec                   |
| Kinetic energy         | $\frac{1}{2}m\dot{z}^2$   | lb-in                   | $\frac{1}{2}J\dot{\theta}^2$  | lb-in                       |
| Potential energy       | $\frac{1}{2}kz^2$   | lb-in                   | $\frac{1}{2}K\theta^2$  | lb-in                       |
| Work                   | $\int F dz$   | lb-in                   | $\int T d\theta$  | lb-in                       |
| Natural frequency      | $\omega_n = \sqrt{k/m}$   | rad/sec                 | $\omega_n = \sqrt{K/J}$   | rad/sec                     |
| Equation of motion     | $m\ddot{z} + c\dot{z} + kz = F_0 \sin \omega t$   |                         | $J\ddot{\theta} + \gamma\dot{\theta} + K\theta = T_0 \sin \omega t$   |                             |
| Initial conditions     | $z(0) = z_0, \dot{z}(0) = \dot{z}_0$  |                         | $\theta(0) = \theta_0, \dot{\theta}(0) = \dot{\theta}_0$  |                             |
| Transient responses    | $z_t = Ae^{-\omega_d t} \sin(\omega_d t + \phi)$<br>$\omega_d = \sqrt{1 - f^2} \omega_n$    |                         | $\theta_t = Ae^{-\omega_d t} \sin(\omega_d t + \phi)$<br>$\omega_d = \sqrt{1 - \zeta^2} \omega_n$           |                             |
| Steady state responses | $z_p = X \sin(\omega t - \psi)$<br>$X = \frac{F_0}{\sqrt{(k - m\omega^2)^2 + (c\omega)^2}}$ |                         | $\theta_p = \phi \sin(\omega t - \psi)$<br>$\phi = \frac{T_0}{\sqrt{(K - J\omega^2)^2 + (\gamma\omega)^2}}$ |                             |

As the equation is expanded and generalized for typical rotating machine systems, the equation increases in complexity. The time varying torque can result from the pressure variations in the cylinder of an internal combustion engine or the torque variations imposed upon a turbine wheel as its blades pass the nozzle in a steam or gas turbine.

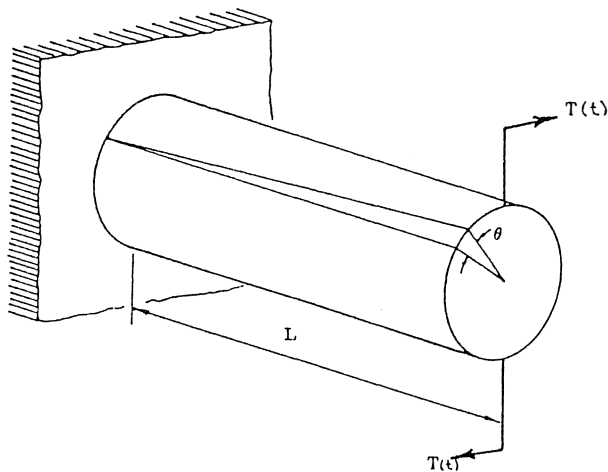


Figure 6. Shaft Section in Torsion.

The first step in analytically determining the torsional response is to calculate the torsional natural frequencies of the system. The stiffness and the mass inertia of the shaft elements must be determined. The equation for  $\theta(t)$  relates the elastic properties of a shaft to the imposed dynamic torques. The shaft stiffness can be determined from these elastic properties. The equation for shaft stiffness,  $K$ , of a uniform section is  $K = I_p (G/L)$ , (in-lb/radian). Mass inertia (commonly called  $WR^2$  but, properly,  $MR^2$ ) of a solid cylinder or disc can be calculated by the following equation:

$$J = \frac{1}{2} MR^2, \text{ in-lbs-sec}^2 \quad (2)$$

Equations for stiffness and mass inertia calculations for common shapes are given by Blevins [5].

The torsional natural frequency of the torsional pendulum can be calculated by the following equation:

$$\omega_n = \sqrt{\frac{K}{J}} = \sqrt{\frac{2I_p G}{LMR^2}} \quad (3)$$

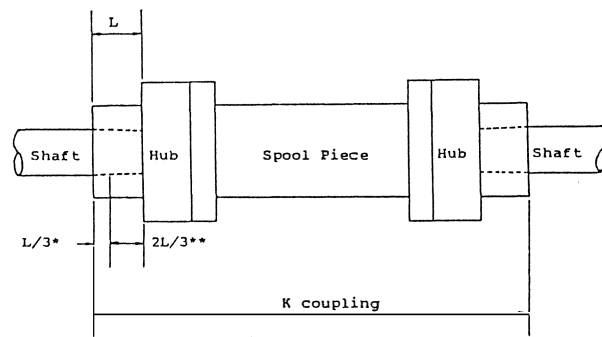
The preceding equation is limited to a uniform shaft with one end fixed and the other end free with an attached rotating mass which is a simple torsional pendulum. The same theory can be generalized to a shaft system of any complexity with any number of rotating masses.

The torsional natural frequencies of simple systems can be calculated by a simple equation [5]; however, the analysis of more complex systems requires additional details for each specific component.

### Modelling

To calculate the torsional resonant frequencies of a system, a mathematical model is synthesized which responds in the same manner as the actual system. All of the mass-elastic and damping properties of the system are required to assemble this mathematical model. The calculations required to determine shaft stiffness and the mass inertia are straightforward. These calculations become complex if the system either has many stepped shafts and rotating masses or when the shaft ceases to be cylindrical, as in the case of an internal combustion engine crankshaft.

The accuracy of the analysis depends upon how well the actual assembly of components matches assumptions. The shaft stiffness at the coupling is based on a typical assumption as shown in Figure 7; however, the effective stiffness of that section of the shaft depends on the actual coupling-to-shaft shrink fit. Another source



- \* Shaft twists freely for L/3
- \*\* No slippage for 2L/3

Figure 7. Coupling Shaft Penetration Assumption.

of calculation errors is in the polar mass inertia of complex shapes such as compressor impellers, turbine wheels, and motor armatures. The mass-elastic properties and the mass inertias can be calculated, measured or obtained from the manufacturer of the specific components. The rotating masses are represented by a series of lumped torsional inertias connected by torsional springs which represent the shaft stiffnesses between the torsional mass inertias.

### Torsional Inertias

Each significant polar mass moment of inertia should be considered in the analysis. Typical inertias include: motor and generator rotors, turbine wheels, coupling hubs, compressor or pump impellers, gears, and crankshaft webs. Each vendor normally provides the torsional mass moment of inertia values for their equipment components. These inertia values should be checked prior to the computer analysis. Formulas for calculating the polar moment of inertia for selected configurations are given by Blevins [5]. The polar moments of inertia are sometimes called  $Wk^2$  values, where  $k$  is defined as the radius of gyration. The radius of gyration is not equal to the radius of the shaft. For example, the radius of gyration ( $k$ ) for a cylinder is equal to 0.707 times the shaft radius, ( $R$ ).

If European manufactured equipment is involved in the system, be aware that their equation for mass inertia,  $GD^2$ , may be based on the diameter and not radius of the mass. Therefore, the values an European manufacturer gives may be four times larger than the value consistent with the analysis using  $WR^2$  which may cause confusion. It is important to verify the basic equation and units used to calculate the mass inertia.

### Torsional Stiffnesses

**Shafts:** The torsional stiffnesses between masses (torsional inertias) are normally calculated from dimensioned shaft drawings. The stiffness of a uniform diameter shaft is equal to  $I_p (G/L)$  where  $I_p$  is the polar area moment of inertia,  $L$  is the shaft length, and  $G$  is the shear modulus of the shaft material. An equivalent shaft stiffness is calculated for shaft sections with diameter changes between masses. The effective spring constant ( $K_e$ ) is determined by  $1/K_e = 1/K_1 + 1/K_2 + 1/K_3 + \dots$  where  $K_1$ ,  $K_2$ , and  $K_3$  are the spring constants for stiffnesses calculated for the cylindrical sections. The shaft torsional stiffness provided by the manufacturer is often from the shaft center to the shaft end and may not be the value needed for the torsional model. The equations for calculating the torsional stiffnesses of several cross sectional shapes are given by Blevins [5].

**Couplings:** Couplings are typically modelled with a torsional inertia at each hub of the driven and driving equipment connected by the coupling stiffness. The torsional stiffness of couplings obtained from the manufacturer is normally used since experience

indicates good correlation using their data. "Certified coupling drawings" from the vendor are recommended to ensure that the torsional analysis is made with the correct couplings. For coupling stiffness calculations, the vendor usually assumes one-third penetration of the shaft into the hub, which means that two-thirds of the shaft length in the hub has no relative motion (Figure 7). This assumption should be confirmed with the vendor prior to modeling the system. The stiffnesses of the adjacent shaft sections are thus simulated up to the edge of the coupling hub. The stiffness contribution of shrink or hydraulically fitted coupling hubs can be analyzed for specific cases.

Couplings with elastomeric elements in compression have a nonlinear stiffness which depends upon the actual transmitted torque through the coupling. As a system starts, and the speed increase results in a load increase, some the torsional natural frequencies will change (Figure 8). Notice that the torsional natural frequency parallels the  $1 \times$  speed line, causing the speed to be near resonance for a wider range. It is possible that the speed could coincide also with the torsional natural frequency over a speed range. A solution that worked favorably in this instance was to increase the rubber durometer of the elements in the coupling. In constant speed systems experiencing load variations, the coupling stiffness can increase and cause the torsional natural frequency to shift.

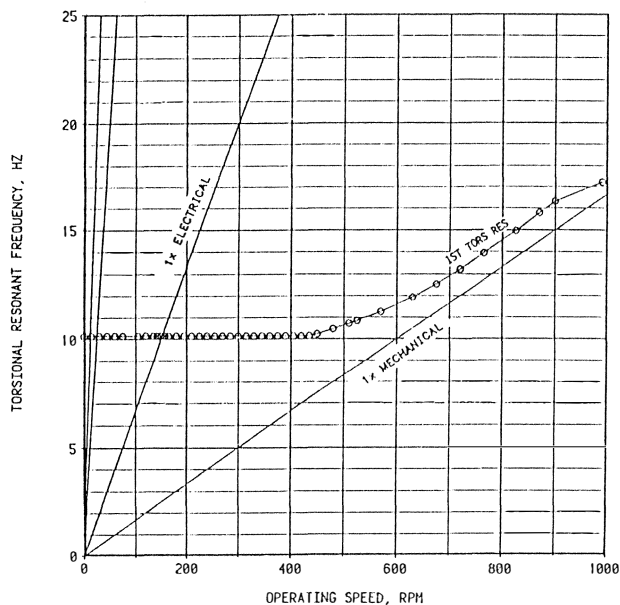


Figure 8. Effect Of Variable Stiffness Coupling on Torsional Natural Frequencies.

Couplings with elastomeric elements in shear have a constant stiffness which is independent of the transmitted torque through the coupling. Some couplings have steel springs in compression in a circumferential orientation, to create a more resilient coupling.

**Gear Teeth:** In geared systems, the equivalent gear mesh torsional stiffness is high compared to the torsional shaft stiffnesses, and has minor influence on the lower torsional natural frequencies which are the ones of concern in most system torsional problems. However, the gear tooth stiffness still should be correctly modelled to predict all the torsional natural frequencies accurately. The gear mesh stiffness can have a significant effect in systems with multiple gear sets. The gear tooth stiffness can be calculated from the gear tooth geometry by considering the effects of tooth bending, tooth shear deflection, and surface compression [2].

**Geared Systems:** Special techniques are required to handle multibranch geared systems and transmissions. Torsional analysis programs should be able to simulate multibranch geared systems which may occur in compressor trains, marine propulsion systems or engine transmissions. The most common method of modelling systems of this type is to generate an equivalent system. In the equivalent system, the shaft stiffnesses and torsional inertias may be adjusted so that the proper natural frequencies are calculated. The torsional inertias and stiffnesses of one branch can be multiplied by the speed ratio squared.

$$I_2' = I_2 \left( \frac{N_2}{N_1} \right)^2 ; K_2' = K_2 \left( \frac{N_2}{N_1} \right)^2$$

(where  $N_2$  and  $N_1$  are the speed of branches 2 and 1, respectively.) If the gear teeth are considered rigid, the equivalent pinion and bull gear inertias can be combined. However, the actual system including gearing effects (tooth stiffness and individual gear and pinion inertias) should be modelled. This is particularly important in high speed systems where excitation frequencies could be near the modes sensitive to tooth stiffness, or in systems with multiple gear sets or branches.

This simplified technique is valid only in systems with fixed gear ratios. Epicyclic gear trains with feedback loops have varying speed ratios and different techniques must be used.

#### Damping

The torsional system damping can be modelled with modal damping (i.e., a damping value for each natural frequency), or discrete damping of any particular element can be simulated, such as torsional dampers or elastomeric couplings.

The system modal damping is related to the resonant amplification factor, AF, by the equation  $AF = 1/2\zeta$  where  $\zeta$  is the critical damping ratio. The AF value defines the sharpness of the resonant response; values ranging from 20 to 30 are typical of machinery torsional resonances. This corresponds to a damping value of 2.5 to 1.67 percent of critical damping. Modal damping, derived empirically from numerous field measurements on machinery system, is utilized with the applied forcing torques to calculate the torsional amplitudes and stresses.

An elastomeric coupling can add damping to a system and can be particularly effective in reducing stresses in some low modes that have twisting through the coupling. The elastomeric coupling is typically flexible and may lower the torsional natural frequency.

#### Calculation of Torsional Natural Frequencies and Mode Shapes

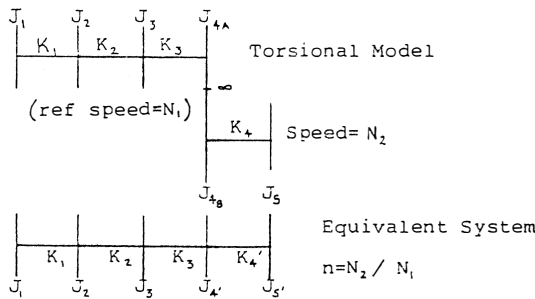
A procedure for calculation of the torsional natural frequencies of a machinery system was developed by Holzer in the early 1900s. Although originally developed as a convenient hand calculation procedure, the method, based on an iterative solution, is readily adaptable to computer analysis. An example using the Holzer analysis is presented in the APPENDIX.

Matrix methods which utilize an eigenvalue/eigenvector solution (sometimes called modal superposition) provide the most versatile analysis technique [6]. This is a practical and accurate method for calculating the torsional resonant frequencies and mode shapes. The forced vibration response can be calculated at any speed throughout the operating speed range. With this analysis, stress levels can be calculated for various levels of dynamic torques (excitation forces) and compared to a failure criterion.

The eigenvector/eigenvalue matrix technique is a closed-form solution that calculates the torsional natural frequencies and vibration mode shapes by directly solving the differential equations of motion for the lumped mathematical model of the torsional system. The development of the differential equations for a five inertia torsional system is illustrated in Table 3.

Table 3. Equations of Motion for Torsional Model.

$$\begin{aligned}
 J_1 \ddot{\theta}_1 &= K_1 (\theta_2 - \theta_1) \\
 J_2 \ddot{\theta}_2 &= K_1 (\theta_1 - \theta_2) + K_2 (\theta_3 - \theta_2) \\
 J_3 \ddot{\theta}_3 &= K_2 (\theta_2 - \theta_3) + K_3 (\theta_4 - \theta_3) \\
 J_4 \ddot{\theta}_4 &= K_3 (\theta_3 - \theta_4) + K_4' (\theta_5 - \theta_4) \\
 J_5 \ddot{\theta}_5 &= K_4' (\theta_4 - \theta_5) \\
 J_4' &= J_{4A} + n^2 J_{4B} \\
 J_5' &= n^2 J_5 \\
 K_4' &= n^2 K_4
 \end{aligned}$$



In matrix notation, the system of differential equations including damping is:

$$[J]\{\ddot{\Theta}\} + [C]\{\dot{\Theta}\} + [K]\{\Theta\} = 0 \tag{4}$$

- where [J] = diagonal inertia matrix
- [K] = stiffness matrix
- [C] = damping matrix
- {Θ} = angular displacement vector, radians
- {Ḑ} = angular velocity vector, radians/sec
- {Ḑ̈} = angular acceleration vector, radians/sec<sup>2</sup>

Normally, the damping in torsional systems with steel couplings is small and has little effect on the natural frequencies. Therefore, the torsional natural frequencies and mode shapes may be calculated, assuming the damping is zero. The equation is simplified since the damping matrix [C] = 0. The solution of these equations can be obtained by assuming simple harmonic motion.

$$\Theta = \Theta \sin \omega t \tag{5}$$

The matrix equation can be reduced to

$$[J][\omega^2]\{\Theta\} = [K]\{\Theta\} \tag{6}$$

where  $\omega^2$  represents the diagonalized eigenvalue matrix. The matrix equation for a five mass system is given in Table 4. Since J is a diagonal inertia matrix, its inverse is readily obtained by forming a matrix whose diagonal is the individual inverse of the individual inertias. By multiplying both sides of the matrix equation by J inverse  $[J]^{-1}$ , now:

$$[\omega^2]\{\Theta\} = [J]^{-1}[K]\{\Theta\} \tag{7}$$

Bringing both terms to the left side, there is

$$([J]^{-1}[K] - [\omega^2])\{\Theta\} = 0 \tag{8}$$

This form of the matrix equation is the well known eigenvalue equation. The values for  $\omega^2$  for which the equation is soluble are known as the characteristic values, or eigenvalues, of the matrix. Correspondingly, the vector solutions for {Θ} are the eigenvectors of the matrix  $\{J^{-1}K\}$ , which are referred to as the stiffness-mass matrix.

The solution of this problem requires that the determinant of the coefficient matrix vanish since {q}, which represents the eigenvector, must be a nonzero quantity. The equation obtained from the determinant of the coefficient matrix is known as the characteristic equation of the matrix, and the values of w for which the equation is satisfied are the desired eigenvalues. In general, the characteristic equation will have "n" roots with "n" corresponding eigenvectors.

Physically, these eigenvectors represent the mode shape of vibration corresponding to the eigenvalue or resonant natural frequency. Each eigenvector is normalized with the maximum amplitude equal to 1.0 and plotted to illustrate vibration mode shapes (Figure 1). On resonance, the vibrational pattern will match one of the eigenvectors; however, if the forcing frequency occurs away from a natural frequency, the pattern will be a combination of the modes above and below the operating speed.

After the natural frequencies are calculated, they can be plotted on an interference diagram (Figure 9), which is a graphical method of checking for a coincidence of the torsional critical speed with an operating speed or its multiples.

Table 4. Matrix Equation of Torsional System.

$$\begin{bmatrix}
 1 & 0 & 0 & 0 & 0 \\
 0 & J_2 & 0 & 0 & 0 \\
 0 & 0 & J_3 & 0 & 0 \\
 0 & 0 & 0 & J_4 & 0 \\
 0 & 0 & 0 & 0 & J_5
 \end{bmatrix}
 \begin{bmatrix}
 \ddot{\theta}_1 \\
 \ddot{\theta}_2 \\
 \ddot{\theta}_3 \\
 \ddot{\theta}_4 \\
 \ddot{\theta}_5
 \end{bmatrix}
 + \dots
 \begin{bmatrix}
 K_1 & -K_1 & 0 & 0 & 0 \\
 -K_1 & K_1 + K_2 & -K_2 & 0 & 0 \\
 0 & -K_2 & K_2 + K_3 & -K_3 & 0 \\
 0 & 0 & -K_3 & K_3 + K_4 & -K_4' \\
 0 & 0 & 0 & -K_4' & K_4'
 \end{bmatrix}
 \begin{bmatrix}
 \theta_1 \\
 \theta_2 \\
 \theta_3 \\
 \theta_4 \\
 \theta_5
 \end{bmatrix}$$

Since the torsional natural frequencies are a function of the mass and stiffness of the system, adjustments in the stiffness or mass of an element can usually shift the resonant frequencies, as required. For most systems, the couplings can be adjusted easily, even if the major equipment components are under manufacture or have been completed. If a 10 percent margin cannot be attained, then particular care must be taken in predicting the forced response of the system, assuming conservative forcing functions at the resonant frequency.

**FORCED RESPONSE ANALYSIS**

The eigenvalue method for calculating the torsional natural frequencies and mode shapes allows for the calculation of the forced vibration response of the system due to various forcing functions at different mass locations, including the phasing of all forces. An n-harmonic Fourier expansion of the forcing function can be applied at each mass location. A steady-state forced response analysis includes the dynamic torques and the interaction of the system while at steady operating conditions. The exciting torques that must be considered may be at frequencies that include shaft operating speeds, multiples of speed, blade passing frequen-

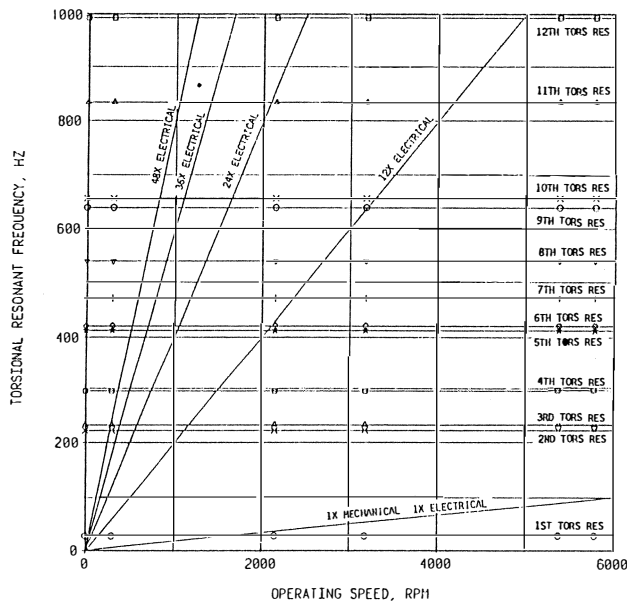


Figure 9. Interference Diagram of Centrifugal Compressor Train.

cy, electrical frequency and its harmonics. In this manner, complex forcing functions with as many harmonics as desirable (i.e., internal combustion engines or reciprocating compressors) can be used in the forced vibration solution of the problem.

When all of the mass and elastic properties in the system have been properly determined and the forced vibration solution of the problem has been completed, the angular amplitudes at each mass location are determined. The relative deflection between the masses determines the twist in each shaft and the resulting stress. Stresses in each of the shafts for each of the harmonics can be calculated by utilizing the phase relationship of the various harmonics, and the complex peak-to-peak stress wave can be generated. This allows the calculation of the maximum overall peak-to-peak stress, along with the individual stresses that can result from a particular harmonic.

**Forcing Functions**

Once the system has been modelled and the natural frequencies have been determined, then the forcing functions are applied. The forcing functions represent dynamic torques applied at locations in the system that are likely to generate torque variations. Identification and quantification of all possible sources of dynamic torque is an important step in diagnosing an existing vibration problem or avoiding problems at the design stage.

The torsional response to excitation torques at any or all mass inertia locations can be accurately calculated using an eigenvalue/eigenvector solution technique. The phasing of each forcing function can be considered by using a complex Fourier expansion of the excitation torques. The most likely dynamic torque excitations, the frequencies and magnitude of torque modulation, are listed in Table 5. A brief discussion of the origin of the torques from each of these items will be included in the following sections.

**Reciprocating Equipment**

The conversion of reciprocating power to rotating power through a crank mechanism generates a variable torque because of the geometry of the system (Figure 10). The geometry of reciprocating equipment can be simulated along with the gas pressure caused torques (power or compressor cylinder) to define the dynamic torsional energy introduced into the shaft system. An internal

Table 5. Steady State Torsional Excitation Sources.

| Source                           | Frequency   | Amplitude % $\tau_{SS} 0-p$                     | Comments  |
|----------------------------------|---|---|---|
| Centrifugal Compressors          | 1x  | 1.0%  | Misalignment  |
| Turbines                         | 2x  | $\frac{1}{2}$                                   |   |
| Pumps, Fans                      | $Bx, \beta x$<br>$B = \text{Number of Impeller Vanes}$<br>$\beta = \text{Number of Diffuser Vanes}$ | $(\frac{1}{B})\%$<br>$\frac{1}{\beta}\%$        | Assumes No Acoustical Resonances  |
| Gears                            | 1x<br>2x, 3x, nx  | 1%<br>$\frac{1}{2}, \frac{1}{3}, \frac{1}{n}\%$ | Worn Gears, Bad Alignment   |
| Reciprocating Compressors, Pumps | 1x, 2x, nx  | TEC * [1-3]                                     | *Torque Effect Curve (TEC) Must Be Developed for Each Cylinder                        |
| Lobed Blowers                    | 1x, 2x, nx  | 10-40% Typical                                  | Harmonic Torques Depend Upon Number of Lobes and Their Timing                         |
| Engines (2 Cycle)                | 1x, 2x ... nx   | Harmonic Torque Coefficients [1-3]              | Based on Pressure - Time Wave From Power Cylinder Function of Mean Effective Pressure |
| Engines (4 Cycle)                | $\frac{1}{2}x, 1x, 1\frac{1}{2}x, 2x$<br>$2\frac{1}{2}x \dots nx$                                   | Harmonic Torque Coefficients [1-3]              | Based on Pressure - Time Wave From Power Cylinder Function of Mean Effective Pressure |
| Variable Frequency Motors        | 1x, 2x ... nx<br>6x, 12x ... 6nx  | Mfg. Supplied                                   | Depends Upon Type of VFD  |

combustion engine cylinder develops a torque impulse at the time of combustion [2] and then "coasts" through the exhaust and intake strokes. The nature of the combustion process generates many torque components at multiple harmonics of the operating speed. A four-stroke spark ignition engine develops half-harmonics or half-orders due to the firing frequency occurring every other revolution. Some harmonics can be canceled by adjusting firing order or the vee-angle.

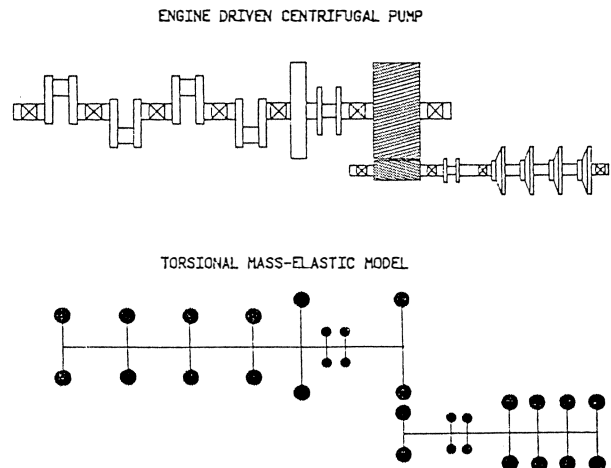


Figure 10. Torsional Model of Reciprocating Equipment.

The excitation torques from the power cylinders of reciprocating engines are a function of the type of engine (two or four cycle, diesel or spark ignition) and the mean effective pressure for the cylinder. The power cylinder harmonic torque coefficients are used to excite the system. The harmonic torque coefficients for four-cycle gas engine types have been generalized in terms of the mean effective pressure [2]. If possible, an actual pressure-time signal from the power cylinder should be obtained so that the amplitudes at all the harmonics can be accurately calculated.

An important effect from the view of torsional vibration is the inertial torque produced by the motion of the reciprocating masses. The inertia of the reciprocating parts creates primary and secondary harmonic torques [3].

Although reciprocating pumps and compressors have a steady discharge pressure resisting the rotation, the changing pressure from suction to discharge level causes a torque variation. Interaction between the pumped fluid and the piping system can produce pressure pulsations that may affect the dynamic torque of the machine and produce higher harmonics.

The torsional excitations generated by reciprocating compressors are a function of the compressor loading condition, the physical geometry of the cylinder, the crankshaft geometry, and the thermophysical properties of the gas or liquid. These harmonic frequency excitations from the complex wave of pressure versus crankangle can be applied at each crank throw with the correct phasing. The shaft angular deflections and stresses between each throw can then be accurately calculated.

In a reciprocating compressor, the excitation torque contribution due to both head and crank ends of each cylinder can be calculated and applied at the appropriate crank rather than having to combine the torques at a single location, such as the flywheel.

The torsional dynamics of any reciprocating machine deserve careful attention because of the multiple frequencies or harmonics. The multitude of frequencies produced increases the probability of exciting a system torsional natural frequency.

#### *Gears*

Gears are a secondary source of torsional excitation which can be minimized by higher quality gears. Torque modulation from good quality gears is usually less than one percent zero-peak of the transmitted torque at  $1\times$  running speed; however, larger percentages have been measured on worn gearsets and bevel gears. Geometrical imperfections caused by the tooth generating process, distortion of the gear, and assembly tolerances can produce significant torsional excitation. Gear unbalance, misalignment, and lateral vibrations of the gear shaft can be translated into torsional excitation. Depending on the mode shape and the gear location, "gear hammer" may occur, which is caused by the gear teeth bouncing through the backlash clearance. Commonly, a dynamic torque excitation at the gear of approximately one percent zero-peak of the transmitted torque is used for geared systems, since field experience has shown this torque to be realistic.

In some geared systems and reciprocating engine systems, the interaction between the lateral and torsional vibrations can be significant. Combined torsional and lateral analyses should be considered for critical applications.

#### *Centrifugal Equipment*

In centrifugal equipment (turbines, compressors, pumps or motors) torsional excitation at the equipment running speed can result from turbulence or load variations, but is generally less than one percent zero-peak of the steady-state torque. Therefore, for  $1\times$  running speed, a one percent torque excitation (zero-peak) is used to calculate the torsional deflections and stresses. The excitation is typically distributed across the masses in the piece of equipment with the maximum calculated amplitude at that frequency to obtain the maximum calculated stress. Torsional excitation can also be applied at other potential excitation locations on the driver, the gear, and the driven equipment. If torsional natural frequencies coincide with multiples of running speeds, the torsional stresses are calculated with an assumed excitation level of  $1/n$  percent of the transmitted torque where  $n$  is the harmonic.

Torsional excitation from centrifugal machines can occur due to the impellers or wheels passing a stationary discontinuity in the case, such as diffuser vanes, steam nozzles, cutwater, etc. These excitations are characterized by a discrete frequency related to the geometry and speed (i.e., vane passing frequency) and rarely exceed one percent zero-peak of the steady load torque unless amplified by acoustic interaction. For cases where blade passing

frequency coincides with torsional natural frequencies, an excitation level of  $1/(\text{number of blades})$  percent zero-peak of steady-state torque is used. Again, these assumed excitations are based on experience and may have to be verified for critical applications.

#### *Motors*

Although, theoretically, there should not be any net dynamic torque component at the electrical frequency for a three phase motor, pulsating torques at motor speed have been documented in torsional tests. While operating at rated speed, motors can produce a fluctuating torque if nonsymmetries exist such as unequal air gaps or unbalanced current in the armature or field. In the calculation procedure, a value of one percent zero-peak has been assumed for  $1\times$  electrical frequency (0.5 percent for  $2\times$ ) and is considered conservative for large hp industrial motors.

Synchronous motors develop a strong oscillating torque during starting because of slippage between the rotor and stator fields [7]. The frequency of the dynamic torque (pulsating torque) is equal to two times the slip frequency and it varies from twice line frequency initially, to zero when the motor speed is synchronized.

Electrical faults can produce braking torques several times the rated torque of the motor. Electrical faults are commonly analyzed for synchronous motors; however, they can occur in any motor or generator.

#### *Couplings*

Misaligned or eccentric couplings can produce a torque fluctuation, particularly if some backlash occurs in gear couplings. The frequency of excitation will be a multiple of operating speed, generally at one and two times. This is similar to the excitation developed by a universal joint which can produce a high second order excitation. A gear coupling can also produce a low level, high frequency, torsional excitation.

#### *Fluid Interaction*

Pulsations within process piping can be produced by the machine (running speed, blade passing frequency) or by the fluid flow excitation and can react on the impeller or wheel to cause dynamic torques on the shaft system [8]. Excitation from flow-induced energy (Strouhal excitation, turbulence, etc.), or from pulsations generated by the machines, can cause the dynamic torques which are typically a fraction of a percent of the nominal load torque. Pulsations in the cylinders and filter bottles of reciprocating compressors can reflect through the pistons to the crankshaft and directly cause torsional vibration.

#### *Load Variations*

Rapid changes in processes which suddenly load compressors or pumps impose a torsional shock or transient upon the system which may excite the lower natural frequencies. A similar occurrence may happen with a turbogenerator system while switching large electrical loads or during motor starts.

#### *Shaft Stresses*

The objective in performing a forced vibration analysis is to evaluate the torsional amplitudes at each mass and the resulting stresses in each shaft. The calculated stresses are then compared to the endurance limit stress of the shaft material to evaluate the probability of fatigue failure.

The torque modulations produced by the prime mover or loaded equipment are applied at the corresponding masses and the resultant stresses are calculated. The torsional stresses in the shafts are dependent upon the applied torques, torsional natural frequencies, stress concentration factors, and the system damping characteristics near the torsional resonances. The shaft stresses are calculated

assuming steady-state conditions; that is, the system operates continuously at each speed.

The torsional shear stresses are based on the relative twist in the shaft between two adjacent torsional mass inertias. The relative deflection (twist) is computed from the eigenvector for each frequency component and recombined to obtain overall peak-to-peak differential amplitudes from the forced vibration response. The torsional stresses in each shaft are dependent upon the amplitudes of the modal pattern. Specifically, the twist ( $\Delta\theta$ ) between each mass, material properties, and shaft dimensions define the torsional stress:

$$S = SCF \frac{GD\Delta\theta}{2L}$$

- where S = stress, psi
- D = minimum diameter, inches
- $\Delta\theta$  = twist between adjacent masses, radians
- L = effective length between adjacent masses, inches
- G = shear modulus of shaft material, lb/in<sup>2</sup>
- SCF = stress concentration factor (dimensionless)

Discontinuities in the shaft (i.e., changes in the shaft diameter, keyways, splines, etc.) between masses produce stress concentration factors (SCF) which amplify the nominal shaft stresses. Stress concentration factors can be determined from the geometry at the discontinuity.

Keyways which comply with the USAS B17.1 code on Keyways and Keyseats [9], have a fillet radius of approximately two percent of the nominal shaft diameter and a stress concentration factor of approximately 3.0. Typical SCF values can vary from 1.1 to 2.0 for stepped shafts and 2.5 to 5.0 for keyways, as shown in Figure 11. If the keyway has a sharp corner at the bottom, the stress concentration factor is significantly greater. Stress concentration factors for other common shaft geometries are given by Peterson [10].

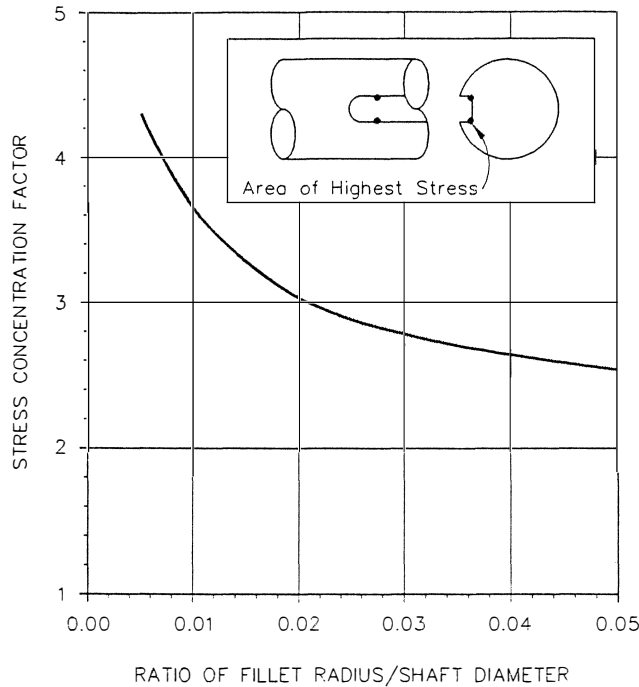


Figure 11. Stress Concentration Factors for Keyways [10].

The torsional combined stress can be determined by combining all of the individual stress harmonics utilizing the phasing of each forcing function. The effect of combining stress components in a shaft for variable frequency drive harmonics is shown in Figure 12 [4].

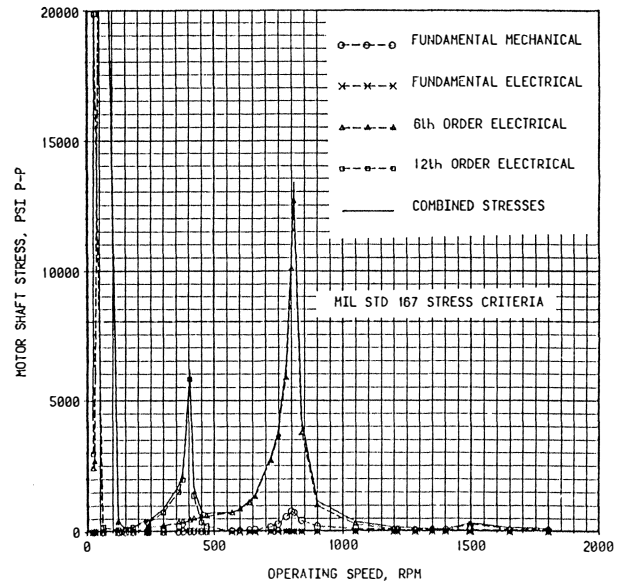


Figure 12. Effect of Combined Stress Orders [4].

Similarly, the coupling vibratory torque can be calculated to determine if it is below the manufacturer's allowable torque. For a transient condition, the instantaneous torque should not exceed the manufacturer's peak torque value.

### TORSIONAL STRESS CRITERIA

The acceptability of the torsional stresses is determined by comparison to accepted engineering criteria. For long term reliability, steady-state calculated torsional cyclic stresses should be compared with the allowable torsional endurance limits for the shafting material to define the safety factor. There is limited published information on the actual torsional endurance limits. Because of the wide variety of steels (composition), it is difficult to determine the fatigue limit for specific material. The strength data can change significantly with heat treatment and fabrication method (i.e., forging). In addition, there are some differences in the interpretation of the allowable torsional stresses with respect to the influence of nominal stress, stress concentration factor, etc.

The purpose of reviewing various criteria is to obtain a general criterion suitable for use as a reference point to identify potential problems. When critical applications are being analyzed, the torsional endurance limit should be obtained for the specific steel composition and heat treatment.

#### US MIL STD 167-2, Type III—Torsional Vibrations

US MIL STD 167-2 [11] defines a torsional allowable endurance stress for steel in paragraph 5.1.2.1.1 *Stresses within speed range*.

“Within the operating speed range, excessive torsional vibratory stress is that stress in excess of  $S_v$  where, for steel,

$$S_v = \frac{\text{Ultimate Tensile Strength}}{25} \quad (9)$$

and for cast iron or other materials

$$S_v = \frac{\text{Ultimate Tensile Strength}}{6} \quad (10)$$

If fatigue tests have been conducted on full scale specimens of the material used, then the contractor may use  $S_v = 1/2$  torsional fatigue limit as the limiting permissible stress.”

The use of  $S_v = 1/2$  of the measured fatigue limit appears to be in recognition of the scatter of measured fatigue data and constitutes a safety factor of 2.

Based upon the US MIL STD 167, the endurance torsional limit of steel is a direct function of the ultimate tensile strength. For instance, a steel with 65,000 psi ultimate tensile strength would have 2,600 psi zero-peak torsional endurance limit. A steel with an 80,000 psi ultimate tensile strength would have 3,200 psi zero-peak allowable and a steel with 130,000 psi ultimate tensile strength would have 5,200 psi zero-peak torsional endurance limit.

Wilson [3] presents a similar equation based on the ultimate tensile strength divided by 22 and states that a safety factor of 2 is included.

*ASME Criteria of Section III [12]*

ASME has developed an allowable stress versus cycles to failure (S-N) curve for low-cycle fatigue analysis for bending stress up to one million cycles (Figure 13). At one million cycles, the fatigue limit in bending is 13,000 psi zero-peak. Based on the theory of maximum shear failure, the allowable shear stress would be one-half the bending fatigue limit, or 6,500 psi zero-peak for carbon steel material with an ultimate tensile strength up to 80,000 psi. For steels with ultimate tensile strength from 115,000 to 130,000 psi, the allowable torsional stress at one million cycles is 10,000 psi zero-peak. If a safety factor of 2.0 is used for comparison to US MIL STD 167, then the allowable torsional stress limit would be 3,250 psi zero-peak, and 5,000 psi zero-peak.

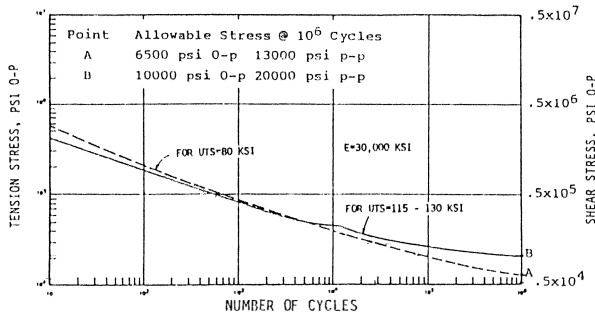


Figure 13. Criteria Of Section III of the ASME Boiler and Pressure Vessel Code for Nuclear Vessels.

*American Society of Metals Handbook [13]*

Based on fatigue tests of AISI-SAE 4340 steel, with a specific heat treatment (annealed), the tensile fatigue limit at one million cycles is given as 55,000 psi zero-peak [13], which would be 27,500 psi zero-peak for a shear fatigue limit stress.

Since these endurance limit stress values are based on polished test specimens, several factors must be applied to provide a reasonable endurance limit for industrial application to shafts. These factors were formulated by Mischke and Shigley [14] to compensate for surface finish, shaft size, reliability, temperature, stress concentration, etc.

$$S_e = k_a k_b k_c k_d k_e \dots \sigma_c$$

$S_e$  = endurance limit, psi

- $\sigma_c$  = fatigue limit of specimen, psi
- $k_a$  = surface finish = 0.8 (machines)
- $k_b$  = size and shape = 0.6 (3" diameter)
- $k_c$  = reliability (usually 1)
- $k_d$  = temperature = 1 (for low temperature)
- $k_e$  = residual stress
- $k_f$  = shock or vibration loading

For typical applications the correction factors would be:

$$k_a k_b k_c k_d k_e = (.8)(.6)(1)(1)(1)(1) = 0.48$$

Applying these correction factors, the allowable endurance stress in shear for AISI 4340 steel would be (27,500)(0.48) = 13,200 psi zero-peak for the 3.0 in diameter specimen. If a safety factor of 2.0 is again used, then the allowable stress limit is reduced to 6,600 psi zero-peak.

When the allowable endurance limits from US MIL STD 167, the ASME criteria, and the ASM data are compared, reasonable agreement is obtained (Table 6).

Table 6. Allowable Torsional Stresses AISI 4340 Steel psi, zero-peak.

| Ultimate Tensile Strength, psi | US MIL STD 167 | ASME Criteria III | ASM 3" Diam. |
|--------------------------------|----------------|-------------------|--------------|
| 80,000                         | 3,200          | 3,250             | —            |
| 130,000                        | 5,200          | 5,000             | 6,600        |

Nominal calculated stress values should be multiplied by the appropriate stress concentration factors and compared to the above allowable stress values.

Although the US MIL STD 167 is a simple, generic criterion, based on the UTS, experience with many systems that have been analyzed and tested has shown US MIL STD 167 to be appropriate (conservative) and is used by the authors. It is an effective criterion for separating systems that will operate reliably from those which could have potential problems. The calculated shear stresses, including the stress concentration factors, are considered acceptable when they are less than the values for the US MIL STD 167 criteria. However, if other stresses are applied simultaneously to the shaft, the resultant stress should be compared to additional criteria for the type of stress (i.e., tensile).

In critical shafting systems, a fatigue limit for the specific steel and heat treatment should be used to generate results with a higher confidence level. For example, extensive testing has been performed on engine crankshafts and criteria have been developed in terms of the combined stresses [15].

As can be seen from the criterion equation, the ultimate tensile strength has a direct relationship to the torsional endurance limit of the shaft material. For systems expected to experience high dynamic torques, such as reciprocating equipment or variable frequency drive motors, good quality steel with higher UTS should be used to provide a higher endurance limit.

**GUIDELINES ON IMPROVING RELIABILITY**

The reliability of systems which are likely to experience large load variations, or torque modulations, can be improved considerably by careful attention during the planning stage to factors which reduce stress or increase the endurance limit of the shaft material. The factors which have the most significant influence on the fatigue life of machine elements are:

- Material—composition, heat treatment.
- Fabrication—method of shaping, surface condition.
- Environment—stress loading, speed, corrosion, temperature.
- Design—size, shape (stress risers), desired life.

In the planning stage, prior to design and manufacturing, these factors can be controlled by specifying the items which will attain the desired life of the machine.

Systems which experience unsteady torque loads (high service factors) as a normal occurrence during startup or operation need all the help possible to withstand the dynamic stresses. Examples of common equipment in industrial plants are:

- Reciprocating engines and compressors
- Adjustable speed motors (variable frequency drive)
- Synchronous motors (startup)
- Generators and motors experiencing electrical faults
- Systems with large inertia

Because high torque loads are expected in these systems, the shaft system must be designed to withstand the imposed dynamic torques. The output shaft size, shaft material and stress concentration factors (keyways, shaft steps) can be specified in the planning stage with minor effect on cost of manufacture, but can save major expense by reducing failure probability.

#### Shaft Size

Many machines have an output shaft diameter which is reduced relative to the journals simply as a cost savings to use a smaller coupling. Because the shaft stress is inversely proportional to the diameter cubed ( $1/d^3$ ), the largest practical shaft diameter should be specified. Extending the journal diameter all the way under the coupling hub will maximize its capability to withstand the dynamic torques. While the larger shaft diameter will provide greater shaft stiffness, a larger coupling would be necessary. Since both stiffness and mass would be increased, the torsional and lateral critical speeds will be affected, and must be considered.

#### Shaft Material

Specifying a better quality steel will pay dividends, because it will have a greater endurance limit and can withstand greater dynamic torques. The heat treatment of typical medium carbon steels also has a significant effect on the endurance limit, as shown in Figure 14. For most steels with hardness index below 400 HB (Brinell), the heat treatment or alloying addition that increases the ultimate tensile strength (UTS) of the steel can be expected to increase its fatigue or endurance limit. The shear endurance limit is related to the ultimate tensile strength of the steel according to US MIL STD 167. The effect of heat treatment on the UTS and the yield strength of two common shaft materials is given in Table 7 [16].

#### Stress Concentration Factors

Stress risers reduce the fatigue strength significantly below the life predicted from tests of smooth test specimen. The stress concentration factor (SCF) for a keyway can range from 2.0 to 5.0, depending on the fillet radius at the base of the keyway. The USAS B17.1 code on Keys and Keyseats [9] recommends a fillet radius of approximately 2 percent of the nominal shaft diameter. A keyway conforming to this code would have an SCF of 3.0 (Figure 11). Generous radii at shaft diameter changes can reduce the SCF as well.

It is common to find existing and new machinery with square cut keyways with no fillet radius. The SCF for a square cut keyway can be 5.0 or greater. The sharp corner has a tendency to initiate a crack

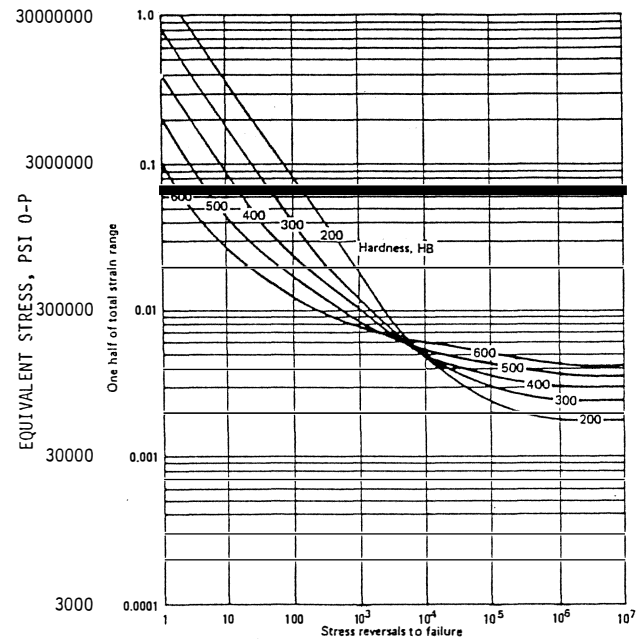


Figure 14. Effect of Hardness on Total Strain Vs Fatigue Life.

Table 7. Strength Properties of Common Steels.

| Steel AISI | Heat Treatment | Brinell Hardness | UTS ksi | Yield ksi |
|------------|----------------|------------------|---------|-----------|
| 1040       | Annealed       | 149              | 75      | 51        |
|            | Normalized     | 170              | 86      | 54        |
|            | Q & T          | 192              | 92      | 63        |
|            | Q & T          | 241              | 110     | 80        |
|            | Q & T          | 262              | 113     | 86        |
| 4130       | Annealed       | 156              | 81      | 52        |
|            | Normalized     | 197              | 97      | 63        |
|            | Q & T          | 245              | 118     | 102       |
|            | Q & T          | 315              | 150     | 132       |

at the corner, as shown in the shaft in Figure 15. Alternate attachment methods, such as hydraulic fits, can reduce stress concentration factors. By minimizing abrupt geometry changes, the SCF can be lowered and the shaft may withstand higher dynamic torques.

#### VARIABLE FREQUENCY MOTORS

One of the major improvements in efficiency of plant operation has been the use of variable frequency drive (VFD) motors. With a variable frequency drive, motor speed can be adjusted for maximum efficiency in the system. Due to the increased operating speed range and additional excitation sources, variable frequency motors require special consideration when analyzed for torsional vibrations.

There are several basic types of variable frequency drive systems, as shown in Figure 16. The most common types used for large horsepower induction motors are:

- *Voltage Source Inverter (VSI)*—The inverter switches the voltage to produce a stepped waveform. At low frequency operation, the current follows the stepped shape of the voltage waveform, but in the mid-frequency and high-frequency range the

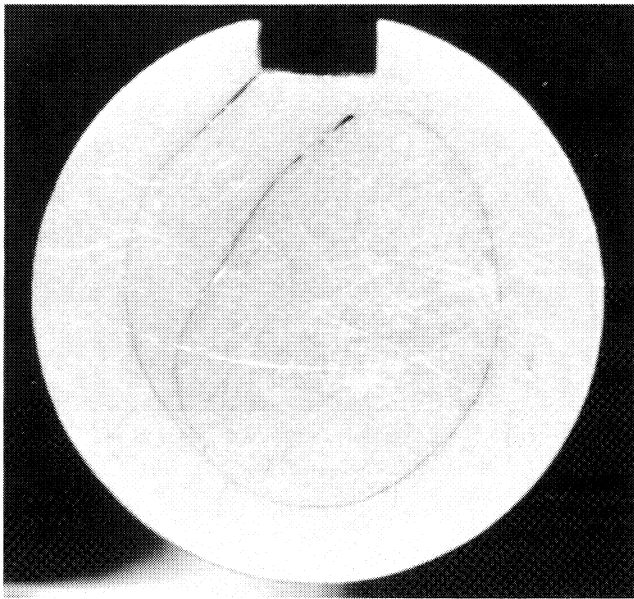


Figure 15. Torsional Failure at Square Cut Keyway.

current waveform approaches a sinusoid and reasonably smooth motor speed is achieved.

- **Current Source Inverter (CSI)**—The inverter switches the current to produce a stepped waveform which, with a greater number of steps, approaches a sinusoid. The stepped waveform results in torque harmonics at multiples of the number of steps.

- **Pulse Width Modulation (PWM)**—High speed switching of the voltage is done to produce a basically sinusoidal current waveform with harmonics related to the high frequency of the voltage pulses.

- **Load Commutated Inverter (LCI)**—This is used with synchronous motors and is similar to the CSI system; however, the circuitry is simpler and, hence, more reliable.

Each of these variable frequency controllers produces harmonic torques at multiples of six times the electrical frequency; however, the amplitude of the dynamic torques vary widely depending upon the characteristics of each type of drive, and the manufacturer's design details.

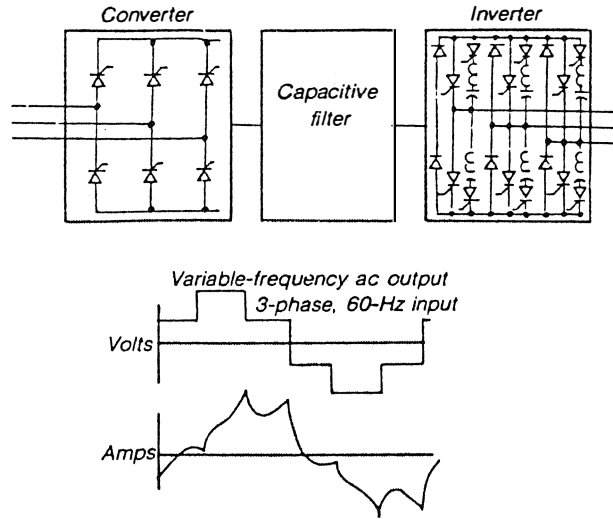
**Excitation Torques**

The torsional analysis for motors utilizing variable frequency drive (VFD) controllers should include the evaluation of the system response to dynamic torques by both the electrical excitation at harmonics of the electrical frequency resulting from the variable frequency drive, and the mechanical excitation at the operating speed. The electrical excitation frequencies should include the fundamental electrical frequency, and 6 ×, 12 ×, 18 ×, ... times the electrical frequency.

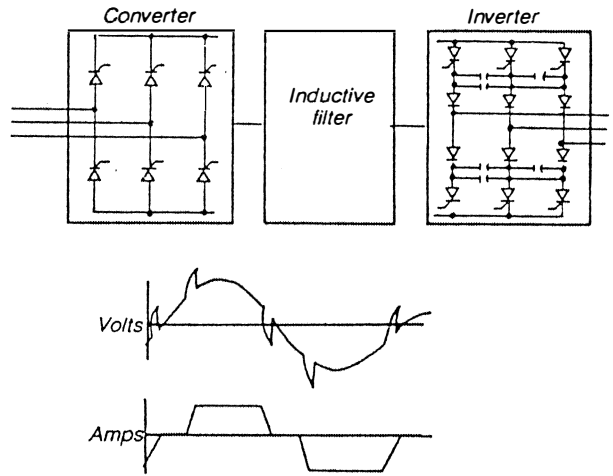
The current source inverter is a common variable frequency drive (VFD) controller that supplies the induction motor with a variable current alternately stepped from positive to negative by means of controlling the timing and gate period of thyristors. This control system produces an "alternating current" with a controllable electrical frequency which normally drives the induction motor at a desired speed from 10 percent to 100 percent of its design speed. The variable DC current is smoothed with an L-C filter consisting of an inductance (including the motor windings) and a capacitor bank.

The stepped current waveform produced by the VFD generates harmonic currents which cause the motor to generate torque

**VOLTAGE SOURCE INVERTER**



**CURRENT SOURCE INVERTER**



**PULSE WIDTH MODULATION**

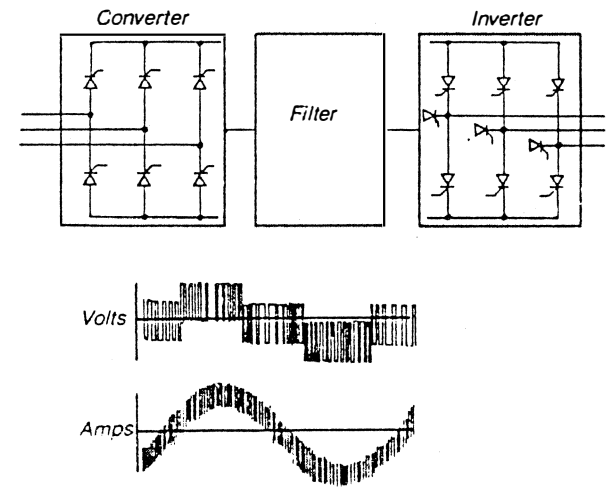


Figure 16. Common Types of Variable Frequency Controllers for Motors.

modulations at  $6 \times 12 \times 18 \times$  the fundamental electrical frequency. The magnitudes of the torque modulations are affected by the resonant frequency of the electrical L-C filter. The dynamic torques generated by the motor as a result of the variable frequency controller ( $6 \times, 12 \times$  electrical frequency) are obtained from the manufacturer during the design procedure for the variable frequency controller.

The fundamental electrical frequency is assumed to have a maximum variation in transmitted torque of one percent zero-peak. Torque modulations may also be produced by mechanical sources in the system. The dynamic torques from mechanical sources in the system can be obtained from Table 5.

#### Interference Diagram

Systems which incorporate VFD controllers require additional considerations in the design stage over conventional constant speed equipment. The wide speed range increases the likelihood that at some operating speed a coincidence between a torsional natural frequency and an expected excitation frequency will exist.

The overall system reliability depends upon the location of the torsional natural frequencies with regard to the potential excitation frequencies. An interference diagram (Figure 9) is generated for the torsional system to identify coincidences between expected excitation frequencies and torsional natural frequencies within the operating speed range. Whenever practical, the coupling torsional stiffness and inertia properties are selected to move the natural frequencies to avoid any interferences within the desired speed range; however, this is usually not possible with VFD systems.

#### Startup

To accelerate any torsional system, the mean torque must be increased to overcome the inertial properties of the system mass. The actual acceleration rate of the system is dependent upon the driver starting torque, the inertias of the equipment, friction and windage loads, and breakaway torque.

In a variable frequency drive system, the dynamic torques at the electrical harmonics are a direct function of the transmitted torque. During startup, an unbalanced torque in excess of the load torque is required to accelerate the system. The larger transmitted torque causes the electrical harmonic torques to increase and may cause higher stress levels than the calculated steady-state values. Faster acceleration rates can cause higher stresses as shown in the startup analysis in Figures 17 and 18. These startup stresses can be calculated by performing a time-domain transient analysis. As the motor starts, all the harmonic orders will usually excite the first torsional natural frequency as shown in the analysis of Figure 19.

For torsional systems in which the inertia of the driven equipment is significantly greater than the motor inertia, the torque modulations from the variable frequency drive may produce stresses in the shafts which exceed the torsional endurance limit during startup. For these cases, the allowable number of starts can be evaluated using cumulative fatigue theory.

### TRANSIENT ANALYSES

After the steady-state analysis is made, a transient analysis can be made to evaluate the startup stresses. The transient analysis refers to the conditions on startup, which are continually changing because of the increasing torque and speed of the system.

#### Startup and Shutdowns

When the system is started and loaded, changes in the static stresses produced by the mean torque must be considered as a low frequency dynamic stress. At the rated speed and full load condition, the driver and driven shafts experience the full transmitted torque. Considering a startup and shutdown (no load to full load

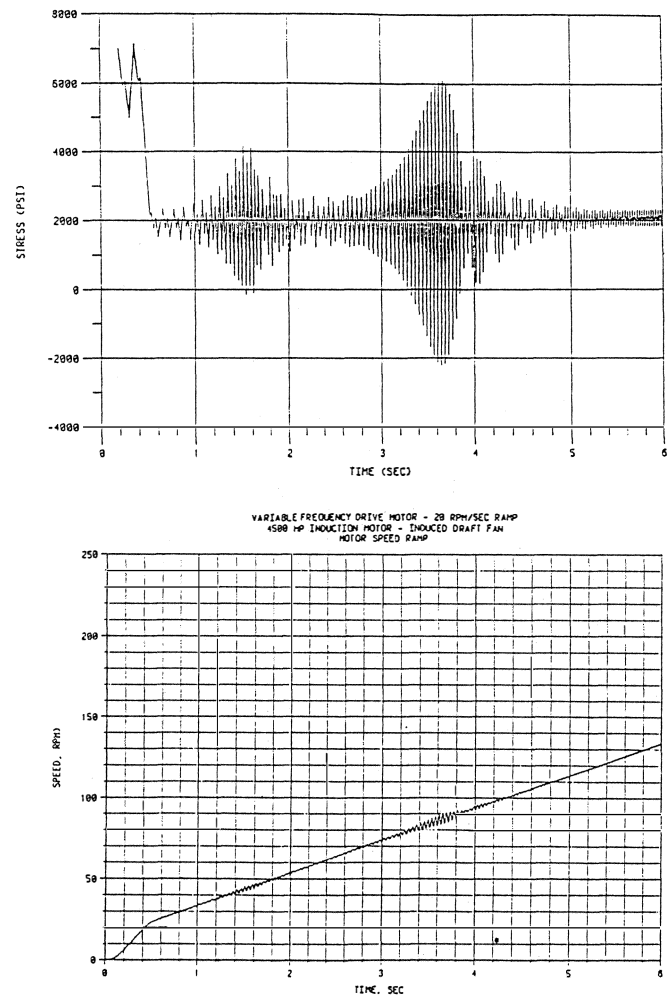


Figure 17. Transient Startup—20 RPM/Sec Ramp.

and back to no load) as a load reversal or cycle, the maximum stress should be calculated (with stress concentration factor) and compared to the shear endurance limit stress. If the shear endurance limit is exceeded, then a cumulative fatigue analysis should be made. Based on the S-N curve for the shaft material, the allowable number of stress reversals (variations from no load to full load) before low cycle fatigue would occur can be estimated for each shaft.

#### Effect of Acceleration Rate on Startup and Shutdowns

Rapid starts increase the rate of acceleration through resonance; consequently, for most systems (except VFD motors) the resonant response would not build up as high (Figure 5) as the calculated steady state stresses, and would lower the peak dynamic stresses. If the startup rate were slower, then the dynamic stresses would be closer to the calculated values based on steady-state assumptions. A transient startup and cumulative fatigue analysis would be required to determine the actual stress levels in the shaft and the allowable startups that the shaft could withstand without fatigue damage.

However, if a system has a large driven mass or large effective inertia (gear speed increaser with large gear ratio), a rapid startup would require a large unbalance torque which would increase the static stress (twist) in the shaft. Slower starts for massive systems may be more acceptable, if the resonances can be avoided.

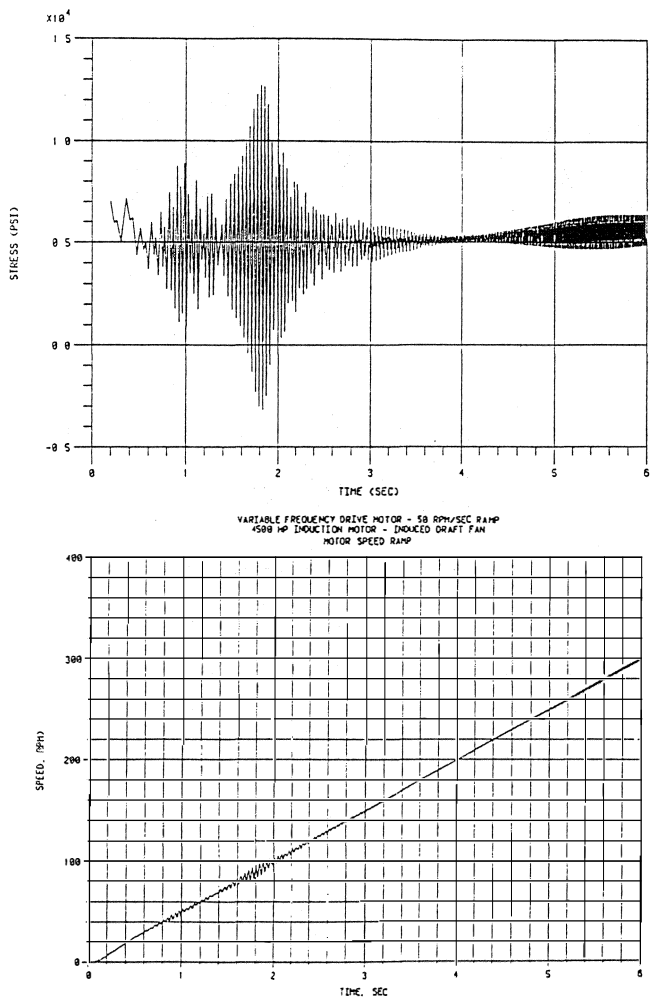


Figure 18. Transient Startup—50 RPM/Sec Ramp.

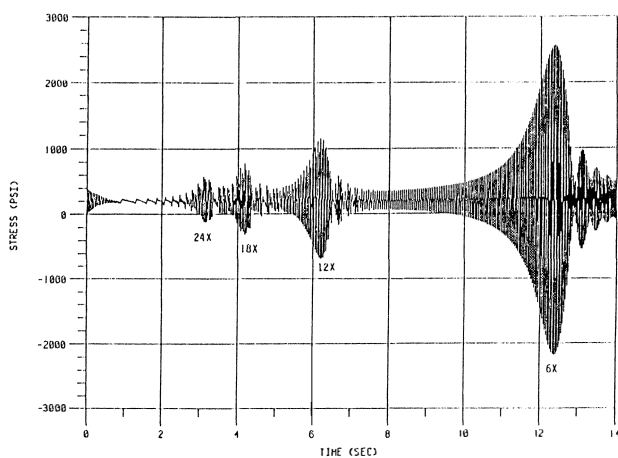


Figure 19. Forced Commutated Mode During Run-up (0 to 300 RPM).

Synchronous Motors

When a synchronous motor starts, an excitation is imposed upon the torsional system due to field slippage [7]. As the motor increases in speed, the torsional excitation frequency decreases

toward zero. During this startup, the torsional system will be excited at its resonant frequencies below 120 Hz. Figure 20 compares the calculated and the measured coupling torque for a 30,000 hp synchronous motor startup. The response amplitude and shaft stresses depend upon the resonant frequencies, the average and pulsating torque when the system passes through these resonant frequencies, the damping in the system, and the equipment load torques. The analyses can be made for startup with the driven machine loaded or unloaded. The transient response is also affected by the starting acceleration rate of the motor. For slower motor startups, the system will stay at a resonant frequency for a longer period of time allowing stresses to be amplified. If acceleration is rapid, then passing through the resonance quickly will minimize the amplification at resonant frequencies.

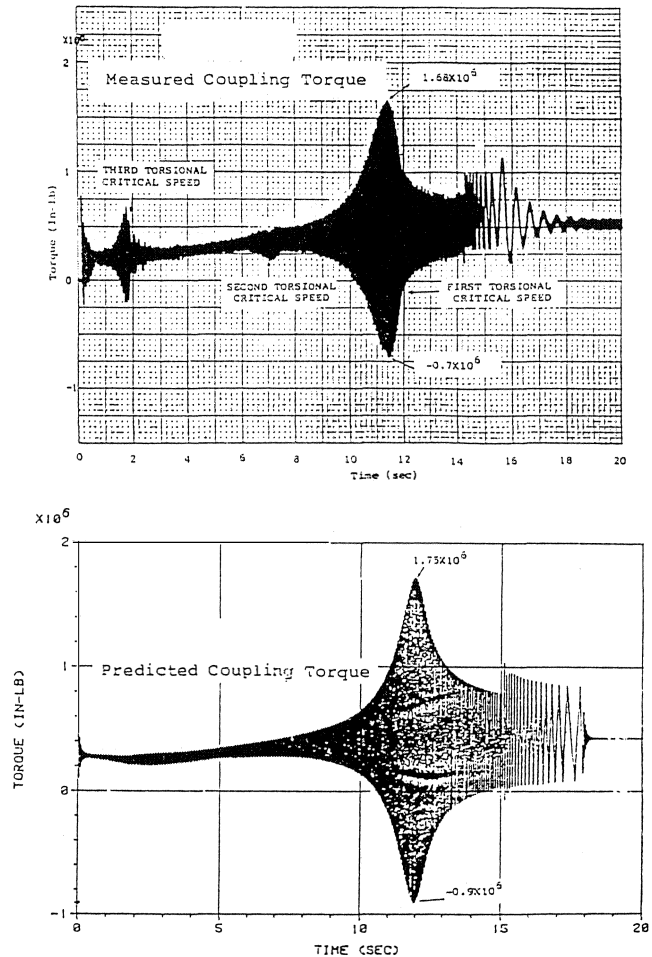


Figure 20. Direct Stress Measurement Of Transient Torsional Startup [7].

Synchronous motors develop a strong oscillating torque during startup because of slippage between the rotor and stator fields. Although this is only a transient excitation, the pulsating torque can be strong enough to exceed the torsional endurance limit of the shaft. For this reason, the transient stresses must be calculated and compared to the endurance limit stress. It is not necessary that the transient stresses be less than the endurance limit stress; however, the stresses must be sufficiently low to allow an acceptable number of starts. If the transient stresses exceed the endurance limit, obtained from the appropriate S-N curve, then the cumulative fatigue analysis is used to evaluate the stresses in excess of the

endurance limit stress to determine how many starts can be allowed for the system.

If the ultimate tensile strength were increased by changing the shaft material, then the allowable number of startups would also increase. However, the number of allowable starts is not a direct linear function of the UTS.

*Short Circuit Analysis*

Short circuit analyses determine the peak transmitted torques, and shaft stresses during fault conditions. For VFD systems, the analyses are performed with the motor speed adjusted, so that the applied electrical frequency is coincident with the torsional resonant frequency to produce the maximum dynamic torque (conservative assumption). The motor air gap torque, as a function of time for the short circuit analyses, is usually obtained from the motor manufacturer. The general form of the equation is:

$$T = Ae^{-at} \sin(\omega t) + Be^{-bt} \sin(2\omega t) + Ce^{-ct} \quad (11)$$

where: T = transient fault torque  
 $\omega$  = electrical frequency, radians/sec  
 A, B, C, a, b, c = constants for specific motor design

*Line-to-Line Short Circuits*

A line-to-line short circuit is a short between two of the phase circuits while the motor is running. It produces a braking torque (Figure 21) which has fundamental and second order frequency components. When analyzing a line-to-line short circuit, the motor should be run with an electrical frequency equal to the torsional natural frequency and also one-half the torsional natural frequency. The analysis should only include frequencies within the electrical frequency range (0 to 60 Hz).

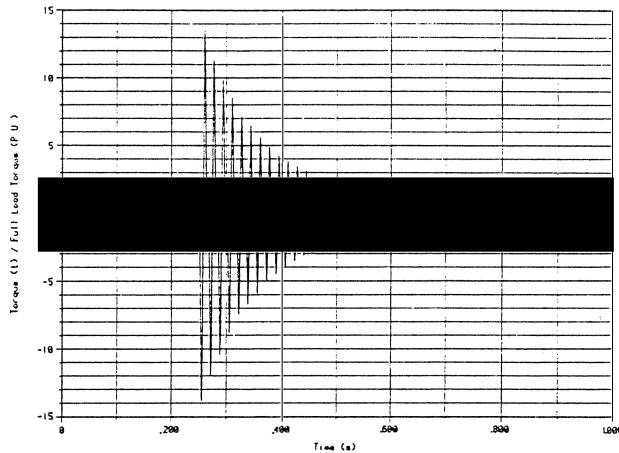


Figure 21. Transient Motor Torque Caused by Electrical Fault.

*Three Phase Short Circuit*

The three phase short circuit would be with all three phases shorted together. It produces a braking torque at the fundamental (no second order).

*Peak Torques*

The peak torques experienced by the motor during a short circuit fault should be converted to stress values (Figure 22) and compared to the shaft material yield strength. This peak torque usually results in maximum torsional shear stresses in the shaft at the keyway under the coupling hub. Under shear loading, the steel will

yield at one-half of the tensile yield strength. If the yield stress is exceeded, local yielding would be expected, normally in the key or at the keyway. Exceeding the peak coupling torque could result in distortion of the coupling torque tube, depending on the safety margin built into the coupling. Macro-yielding of the shaft would not be expected except for gross overloads when the ultimate strength is exceeded. The manufacturer of the equipment and coupling should review the imposed dynamic torques during startup and the peak torques of a line-to-line short circuit. The transient analysis results should be made available to the coupling manufacturer so that the capability of the coupling to withstand the imposed torques can be confirmed.

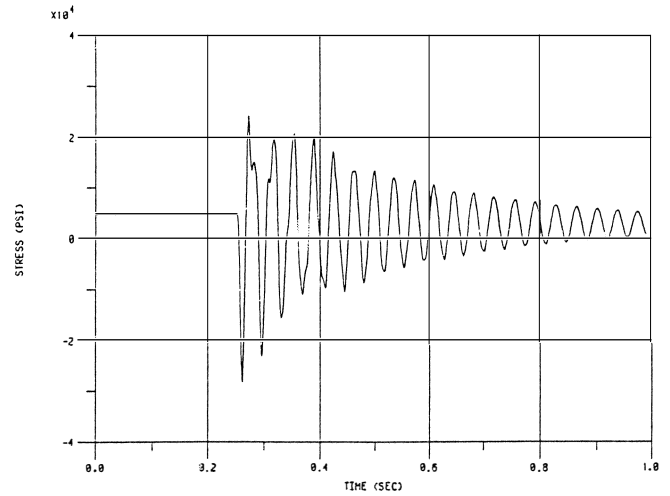


Figure 22. Compressor Input Shaft Stress Caused by Electrical Fault.

If multiple short circuit faults occur, the stresses which exceed the allowable torsional endurance stress could cause fatigue in the shafts. A cumulative fatigue analysis could be made to determine the percentage of fatigue that has been accumulated for a short circuit fault.

*Cumulative Fatigue Analysis*

Since stresses occurring during startup are transient, they should be evaluated on the basis of cumulative fatigue if they exceed the endurance limit. Cumulative fatigue analysis is used to estimate how many cycles of a certain stress level may be endured before shaft failure would occur (Figure 23). The analysis determines the amount of fatigue incurred by each shaft during one startup as a result of stresses in excess of the shear endurance limit. The number of allowable startups can then be determined. In a VFD system, load variations can also result in a significant change in the transmitted torque which constitutes a stress reversal. For instance, changing from full load to minimum load and then back to full load represents a stress reversal which may exceed the shear endurance limit, particularly if stress concentrations are present.

Many different fatigue analysis techniques are available for calculating cumulative fatigue damage. The major differences usually appear in the

- S-N curves,
- Fatigue reduction factors, and
- Stress range counting methods.

An S-N curve based on strain control testing is used since the dynamic portions of the strain or stress variation and yielding are considered. Other S-N curves used for fatigue analysis are the

$\sigma_i$  = STRESS AT  $i^{th}$  CYCLE

$\sigma_e$  = ENDURANCE STRESS

$N_i$  = NO. OF CYCLES TO FAILURE AT  $\sigma_i$

$n_i$  = ACTUAL NO. OF CYCLES AT  $\sigma_i$

$S$  = NO. OF CYCLES TO SYNCHRONOUS SPEED

$$q = \sum_{i=1}^S \frac{n_i}{N_i}$$

$q \leq 1$  = ALLOWABLE NUMBER OF START UPS

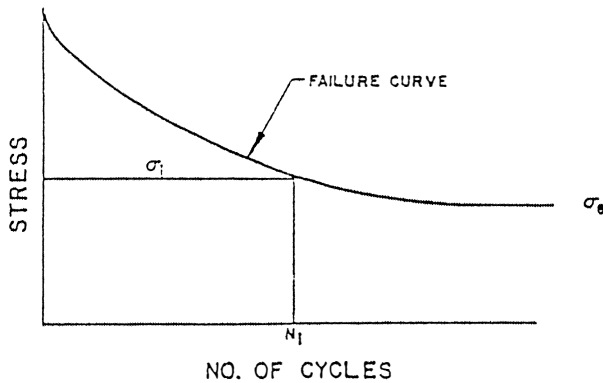


Figure 23. Cumulative Fatigue.

ASME pressure vessel code and the Universal Slopes Method.

Fatigue reduction factors ( $K_f$ ) are usually approximated in the design stage as  $K_r = K_f$ , where  $K_r$  is the stress concentration factor. Accurate values of fatigue reduction factors are difficult to obtain, since they must be experimentally obtained for particular configurations.

Various stress range counting methods can result in significantly different fatigue life estimates. The rain-flow method [17] is a widely accepted technique to evaluate stress cycles and provides reasonable results.

Experimental fatigue tests show that identical specimens have widely different fatigue lives, (factors of 10 are not unusual) and calculations can be used only, at best, as a tool to predict mean life unless conservative S-N curves are used. Various effects also occur in actual machines not accounted for in laboratory fatigue tests, such as surface finish, size, environment, etc. The S-N curve takes into account some of these unknowns, so that a fatigue life prediction should have a safety factor greater than 1.0.

A typical S-N curve used as the design basis to calculate cumulative fatigue for transient torsional analyses is shown in Figure 24. The vertical axis represents the dynamic (alternating) component of stress and the horizontal axis is the number of cycles to failure. It is based on typical shafting steel with an ultimate tensile strength (UTS) of 100,000 psi. The shear endurance limit for the material is necessary to evaluate the cumulative fatigue. However, if the shear endurance limit is not available, an approximate value can be obtained from US MIL STD 167, which defines the approximate shear endurance limit (psi zero-peak) as the ultimate tensile strength, divided by 25.

At high cycles, the S-N curve is defined by the shear endurance limit for one million cycles and above (Point B, Figure 24). At low

cycles, the S-N curve is defined by the ultimate strength in shear. The sloped portion is defined by a line between points A and B. Point A is located at  $10^3$  cycles and 90 percent of the ultimate shear strength. Point C is the intersection of the extension of line AB and the horizontal line at the ultimate shear strength value. The horizontal line between the vertical axis and Point C essentially limits the maximum allowable single alternating stress amplitude ( $S_a = \text{stress range}/2$ ) to the ultimate shear strength.

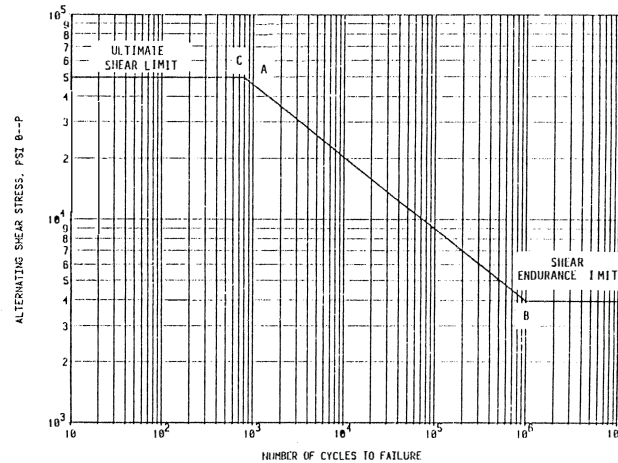


Figure 24. Stress to Number of Cycles to Failure for Shear Stress for Steel With UTS = 100,000 PSI.

The procedure used for calculating cumulative damage during a transient torsional startup is as follows:

- Obtain stress vs time histories using a time-domain torsional modelling technique. Appropriate fatigue strength reduction factors ( $K_f$ ) are applied to the stress-time histories. The nominal stress levels in each shaft must remain in the elastic region (linear model) for the transient torsional analysis to be valid. However, local stress values at stress concentrations may exceed the yield or ultimate strength values.
- Process the stress-time histories using the rain-flow counting method to obtain equivalent stress ranges when numerous stress cycles in excess of the endurance limit occur. These stress ranges represent the dynamic or alternating stress content of the histories.
- Compare the calculated dynamic stresses (zero-peak) to the appropriate S-N curve and calculate the fatigue damage per start using the stress ranges from the rain-flow counting technique and cumulative fatigue theory.

If one stress cycle is described by a minimum stress of -5,000 psi and a maximum of 15,000 psi, the p-p cyclic stress would be 20,000 or 10,000 psi zero-peak for the alternating stress amplitude, and the corresponding cycles to failure would be read from Figure 24 as approximately 75,000 cycles. For transient torsional analyses, the most important stress range determined by the rain-flow counting method is usually the range from the minimum valley to maximum peak, since this causes more damage than any other cycle.

## DIAGNOSING TORSIONAL PROBLEMS

### Recognition of Potential Problems

Recognizing a torsional resonance before excessive damage has occurred is difficult. Torsional oscillations occur as a twisting in the shaft, and can be measured only by the relative motion of rigid masses attached to the shaft. Early warning indicators are exces-

sive gear noise, gear hammer, gear wear, gear tooth failure, coupling failures, slippage of coupling hub, or high gear box structural vibrations. These symptoms can be used to determine if a torsional problem exists before shaft failures occur. Other than these, it requires making direct torsional measurements.

While the equipment is shut down for a routine maintenance check, several things can be investigated that would indicate a high probability of a torsional problem. Gear wear on the unloaded side of the gear teeth should be checked since excessive torsional vibrations would cause impacting of the gear teeth. A similar situation would be indicated by wear on both sides of the coupling teeth. Torsional vibrations occasionally cause loose coupling bolts or fretting corrosion under coupling hubs. Another indication could be poor product quality in roll surface in such products as paper, newsprint rollers, coated plywood, cold steel mills, etc.

If a torsional problem is suspected, the shafts should be checked while the unit is down for the start of fatigue cracks at any changes of geometry where high stress concentrations occur. Minute cracks in such locations of cross-sectional change, particularly at keyways, would warn of impending failure. Torsional failures exhibit a shear crack which propagates along a 45 degree helix.

If a torsional problem is suspected, a torsional investigation including analysis and measurements should be made to define the causes of the problem, the sources of the dynamic torque, and the severity of the vibrations.

#### Measurement Procedures

Available instrumentation to measure torsional natural frequencies, response amplitudes, and the shaft stresses of a system while operating include, a torsiograph rotating with the shaft, strain gauges on a shaft, and frequency modulation systems which use noncontacting pickups on gears (magnetic transducers, proximity probes, lasers, optical transducers).

#### Torsiograph

A torsiograph is an instrument which mounts to the end of a shaft and rotates with the shaft (Figure 25) and is used for measurement of angular displacement or velocity. The most commonly used torsiographs are the CEC torsiograph and the HBM torsiograph. Such torsiographs have a sensitivity of approximately  $\pm 0.1$  degrees. The CEC torsiograph is not in production today; however, it was used extensively during the 1950s to the 1980s. It uses a rotating armature which creates a voltage proportional to the torsional vibrational velocity. The HBM torsiograph is based on the seismometer principle with a mass retained by springs whose

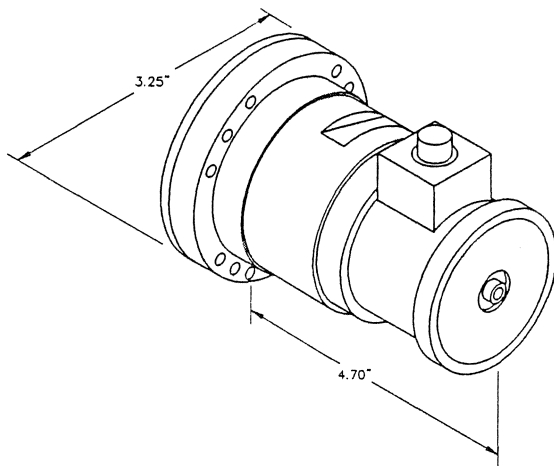


Figure 25. HBM Torsiograph.

relative motion compared to the stator is converted into an electrical signal by inductive proximity detectors. The inside parts of the torsiograph rotate with the system and the outer case is stationary. These devices are mounted on an exposed shaft section of the system.

The torsional signal represents the absolute motion at the point of attachment and can be converted to angular velocity. The data obtained from a torsiograph does not define the seriousness of a torsional vibration. The torsiograph will give a complex wave of the torsional oscillations for one point in the shaft system. Since the stresses are a function of the relative displacement between two masses in the system, the torsiograph data, in itself, does not reveal the stress conditions within the shaft. First, the complex wave should be analyzed by a spectrum analyzer to determine the amplitudes of vibration at each frequency.

Used in conjunction with a mathematical analysis which calculates the normalized mode shape, the measured amplitude from the torsiograph can define the absolute torsional vibration amplitudes at each mass. The relative angular deflections can be calculated and converted into torsional stresses and dynamic torques.

A torsiograph may not give accurate data when used to measure motor starts, because of the rapid acceleration. A torsiograph usually has a peak limit of approximately six degrees pk-pk and a torsional response at 3.0 to 5.0 Hz; therefore, torsional vibrations measured below 5.0 Hz may be in error. The calibration curve for the instrument must be used to obtain accurate data over a wide frequency range.

#### Torsiograph Measurements of Reciprocating Compressor

Diagnosis of repeated oil pump failures required torsional measurement on a six cylinder reciprocating compressor. The torsiograph was attached directly to the end of the crankshaft in place of the oil pump (Figure 26) to measure the torsional amplitudes experienced by the oil pump. An electrical oil pump was used temporarily during the test.

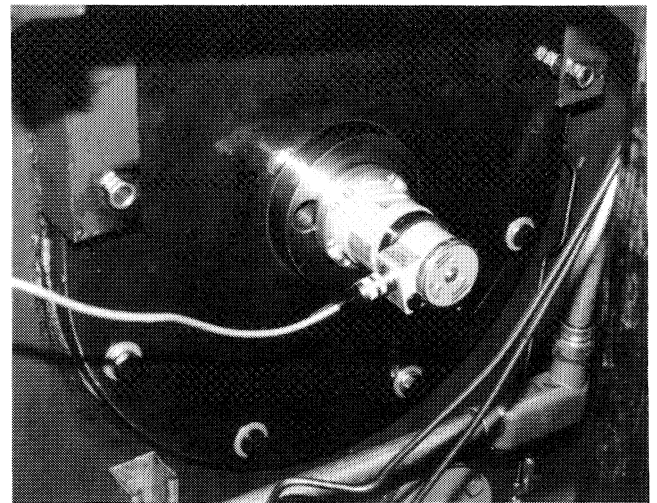


Figure 26. Torsiograph Attached to Compressor Crankshaft.

While loaded 100 percent, the compressor speed was varied from 800 to 1000 rpm and the torsional data was taken. The data is presented in a speed raster format (Figure 27) which shows that the seventh order excited the first torsional frequency (105 Hz) at 900 rpm. As the sixth order approached the resonance at 1000 rpm the torsional amplitude increased to 0.6 degrees pk-pk. Notice that integer orders and half orders occurred because the compressor was driven by a four-cycle spark, ignition engine.

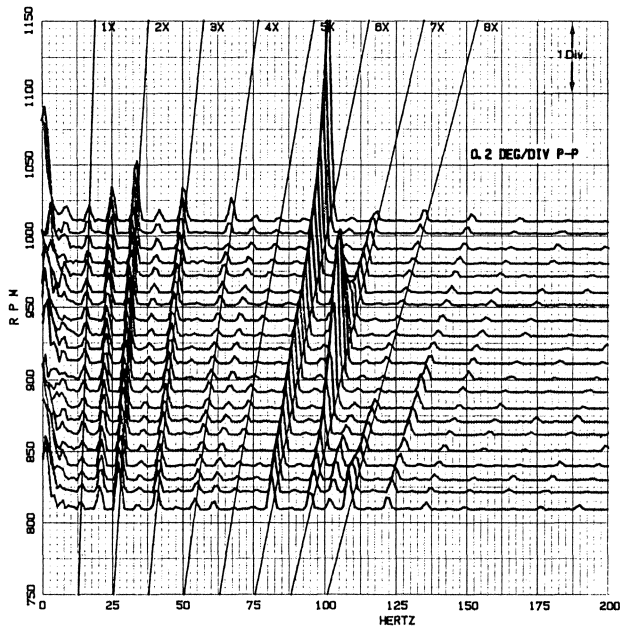


Figure 27. Speed Raster Defining Torsional Resonance.

Frequency Modulation Systems

Frequency modulation (FM) systems use noncontacting transducers to measure the pulse rate or gear tooth passage frequency. Several types of transducers are used to develop the signal which is proportional to the gear tooth frequency. These noncontacting pickups include magnetic pickups, proximity probes, dual beam laser, or optical transducers that monitor the gear teeth or specially produced patterned tape.

These noncontacting pickups with the proper gap setting and sensitivity can indicate gear tooth passage, which can be processed to indicate torsional vibrations. In this method, the pickup basically measures the time or period between the passing of each tooth that produces a frequency modulated (FM) signal (Figure 28). The signal can be demodulated and converted to angular displacement. Relative amplitudes and stresses can be calculated by using the normalized mode shape from the torsional analysis.

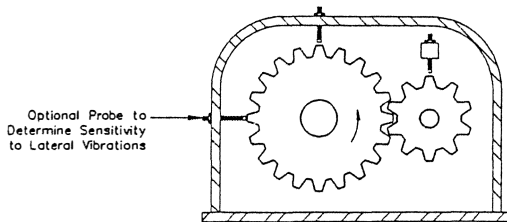


Figure 28. FM Torsional Pickups Installed on Gearset.

The frequency modulation method has several limitations. One is that fictitious torsional signals can be generated by lateral vibrations of the gear and axial vibrations of a helical gear. If the torsional oscillations unload the gear and result in impacting, the signal may be noisy and unusable. The nature of measuring the tooth passing period masks the frequency range around the gear running speed. Because of slight unbalance in the gear (lateral vibrations) the true amplitude cannot be accurately defined unless two pickups 180 degrees apart are used and the signals added. This masking can be compensated for by monitoring noncontacting pickups on both the gear and pinion.

The FM type of measurement system can also be used in a multiple transducer arrangement to measure steady state torque and the dynamic oscillation of a system. This type of arrangement is used in permanently mounted torque meters. The typical arrangement uses three gears on a shaft or coupling with magnetic pickups or proximity probes located on all three gears (Figure 29). The torque in the shaft causes a phase shift between the gears which can be measured from the phase shift with the FM signals [18].

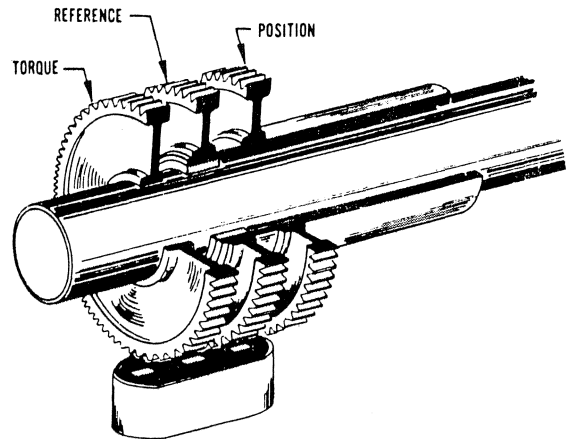


Figure 29. Permanent Torque Meter.

Other schemes that have been used for torsional measurements include using an optical light source which is focused through a slotted wheel [19]. As the shaft is torqued, the light through the slots will be attenuated (Figure 30). When properly calibrated, the torsional vibrations can be obtained. A dual beam laser which monitors the gear passing frequency or a specially developed photo-reflective tape, can be used to measure the torsional vibrations [20].

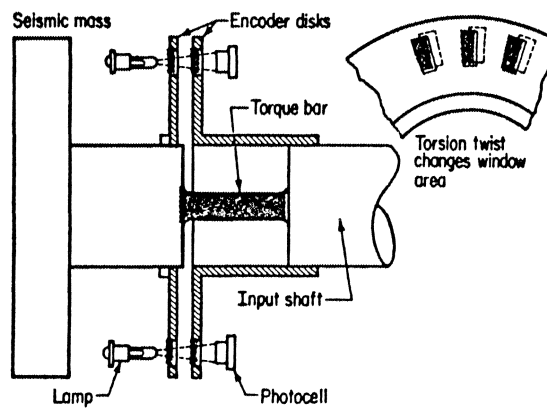


Figure 30. Torsional Measurement Using Photocells and Encoder Disk.

As mentioned above, it is possible to use reflective tape and an optical pickup to generate a FM signal that can be used to obtain the torsional vibrations. This method is somewhat limited in actual field measurement, due to problems caused by the loss of contrast from oil leakage, inexact splicing of the tape, inadequate bonding of the tape, stretching of the tape due to the centrifugal forces, etc. The resolution and accuracy will be limited in many cases.

The FM system data can be processed using a FFT analyzer with a "zoom" mode to develop the side bands adjacent to the gear passing frequency or the tape band frequency. From this data, it is possible to determine the vibration frequency and the torsional vibration amplitudes by using the Bessel function relationships as reported by Vance and French [21].

*FM Measurement of a Diesel Engine*

Two kinds of torsional vibration measurements were made on a diesel engine drive of a lobed blower. A HBM torsigraph was installed on the free end of the engine (Mass 1 on Figure 31) and an FM torsigraph was installed (using magnetic probes) at the bull gear (Mass 13). The torsional natural frequencies and mode shapes are given in Figure 32. The HBM torsigraph measured both torsional natural frequencies (8.9 Hz and 49 Hz), although the amplitudes (degrees) at the first natural frequency were low (Figure 33). The FM torsigraph showed the resonance at 49 Hz; however, the amplitude (degrees per second) at 1x operating speed were highly amplified because of gear lateral vibrations (Figure 34). It was not possible to obtain good amplitude data at the 8.9 Hz resonance at the operating speed of the bull gear.

Because of these limitations, the FM method data is more difficult to interpret than torsigraph data; however, in some installations it may not be possible to install a torsigraph on the free end of a shaft. It is also important to use the proper instrumentation system which utilizes the appropriate electronic filters for the frequency range of interest.

| MASS/ELASTIC DIAGRAM | MASS NO. | WR2<br>in-lb-in <sup>2</sup> | K(1E-6)<br>in-lb/rad | STATION DESCRIPTION |
|----------------------|----------|------------------------------|----------------------|---------------------|
| .....                | 1        | 4.80                         | 235.20               | Crank Gear          |
| .....                | 2        | 99.60                        | 292.50               | Cyl #1              |
| .....                | 3        | 99.60                        | 292.50               | Cyl #2              |
| .....                | 4        | 99.60                        | 292.50               | Cyl #3              |
| .....                | 5        | 99.60                        | 292.50               | Cyl #4              |
| .....                | 6        | 99.60                        | 292.50               | Cyl #5              |
| .....                | 7        | 99.60                        | 292.50               | Cyl #6              |
| .....                | 8        | 99.60                        | 292.50               | Cyl #7              |
| .....                | 9        | 99.60                        | 220.60               | Cyl #8              |
| .....                | 10       | 15400.00                     | 72.40                | Flywheel            |
| .....                | 11       | 76.80                        | 50.40                | Falk Cplg           |
| .....                | 12       | 76.80                        | 294.00               | Falk Cplg           |
| .....                | 13       | 5008.00                      | 58000.00             | Bull Gear           |
| .....                | 14       | 1.94                         | 22.79                | Pinion              |
| .....                | 15       | 2.03                         | 25.10                | Fast Cplg           |
| .....                | 16       | 2.17                         | 11.60                | Fast Cplg           |
| .....                | 17       | 138.88                       | .00                  | Blower              |

Figure 31. Mass/Elastic Data for Diesel Engine Driven Lobed Blower System.

*Strain Gages*

With the use of telemetry (or slip rings) actual strain signals from strain gages attached to the rotating shaft may be obtained. The installation of the strain gages and the telemetry collar or slip rings is more tedious. However, this is the most reliable method for obtaining accurate response frequencies and stresses during a rapid start of a turbine or motor. The direct measurement of

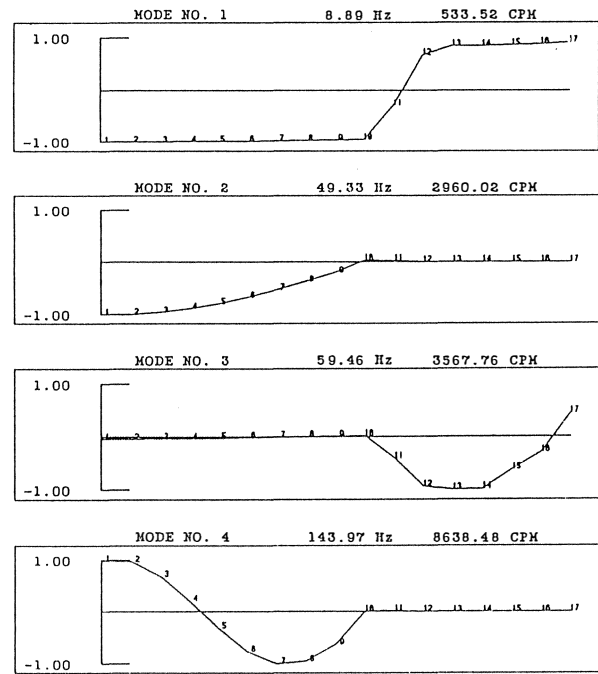


Figure 32. Torsional Natural Frequencies and Mode Shapes.

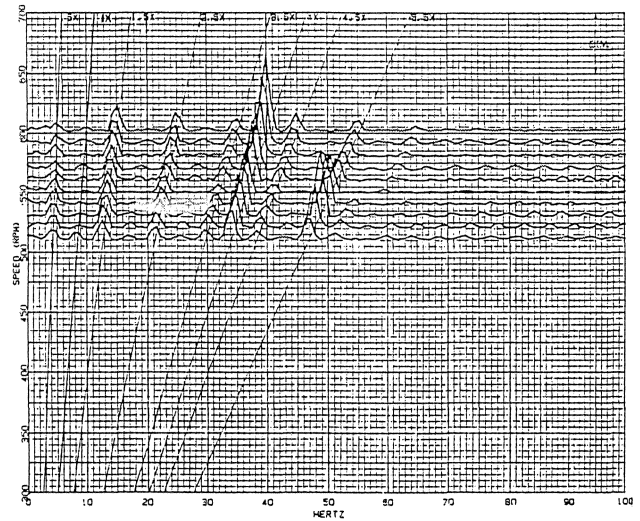


Figure 33. Torsional Vibrations Measured on Engine Free End with HBM Torsigraph.

coupling torque by the use of strain gages during the startup of a 30,000 hp synchronous motor is displayed in Figure 20.

By installing the strain gages in a full bridge circuit (Figure 35), separate signals for axial, torsional, and bending strain can be obtained [22]. The installation of the strain gage and rotating FM transmitter on a motor are shown in Figures 36, 37, and 38. This method can also be used to measure strain of other components such as compressor wheels, turbine blades, etc. Direct measurement of strain using strain gages is the most accurate method for obtaining torsional response.

In all of these measurement methods, stress concentration factors must be included before comparisons to applicable torsional stress criteria are made, since the strain gages are installed away from the stress intensified zone.

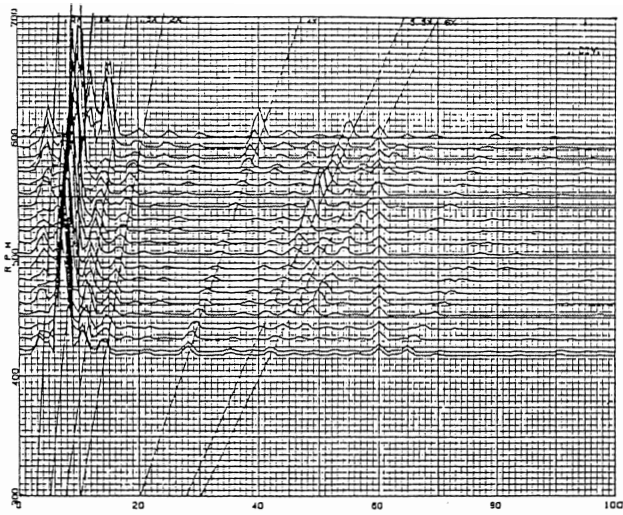


Figure 34. Torsional Vibrations Measured at Gear Box Using FM Torsional Signal from Magnetic Pickup.

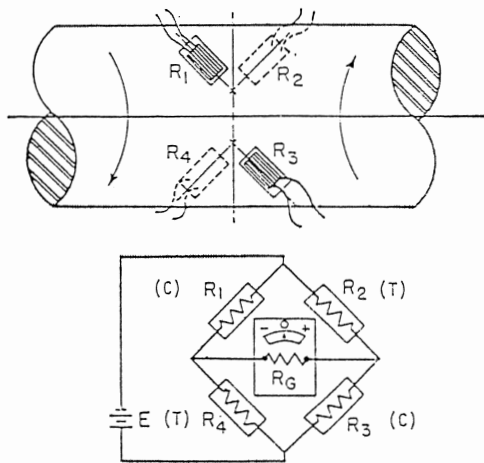


Figure 35. Full Bridge Strain Gage Circuit [22].

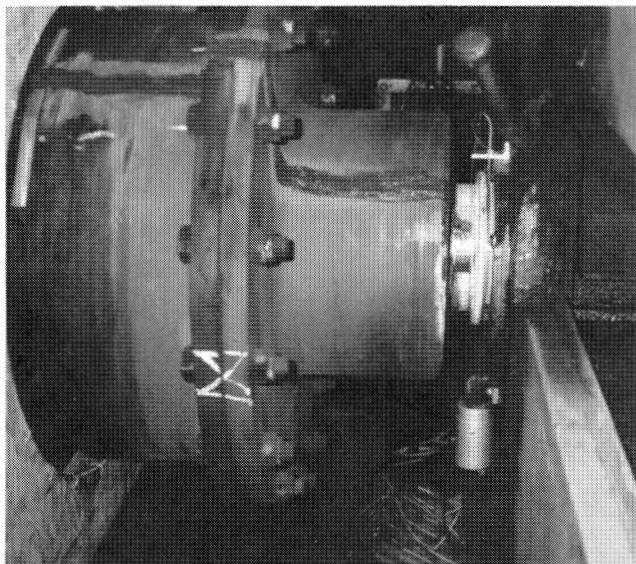


Figure 36. Strain Gage Installed on Motor Shaft.

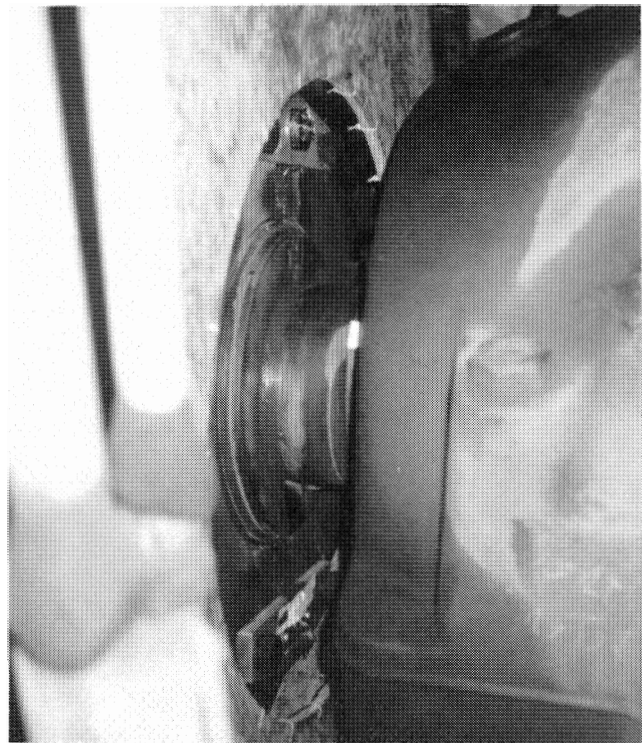


Figure 37. Stationary Antenna Support Around Coupling.

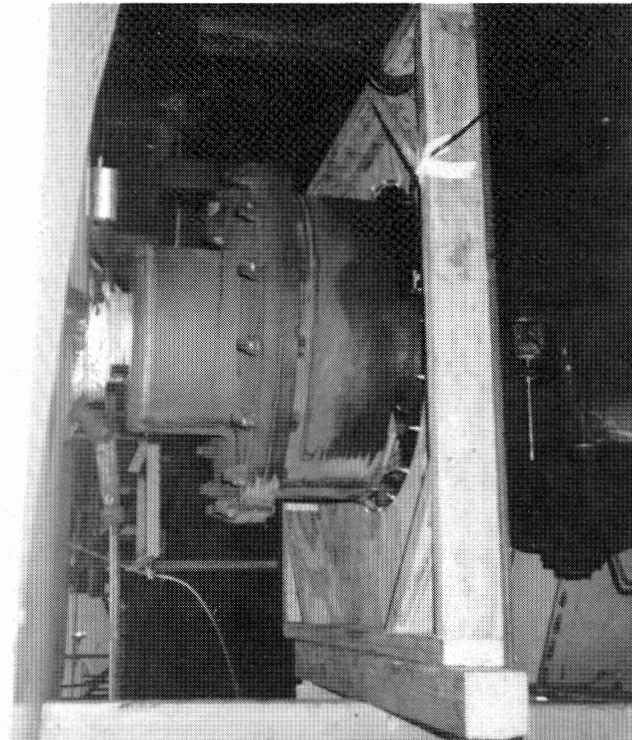


Figure 38. Rotating Transmitter and Batteries Installed on Coupling.

The measured strain is caused by the relative torsional vibrations between the two adjacent masses and is not the same type of information that is obtained from the torsigraph, since that data gives only the torsional oscillations at one location. The conver-

sion of the measurements from the torsigraph or FM method into shaft stress are dependent upon a realistic mathematical model of the system, so that the mode shape can be determined.

*Measurements with Strain Gages on Shaft*

A motor shaft failure occurred on a variable-speed 3000 hp induction motor driving a high speed compressor through a speed increaser (gear ratio; 1:3.44). The system shown in Figures 39 and 40 had few startups and had only operated for 450 hours prior to the failure. The fracture surface exhibited signs of torsion loading; therefore, a complete torsional investigation of the system was

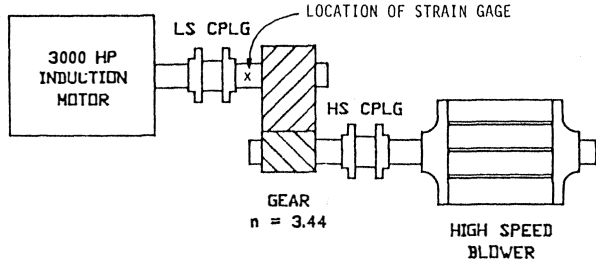


Figure 39. Variable Frequency Drive Motor System.

| MASS/ELASTIC DIAGRAM | MASS NO. | WR2<br>in-lb-g <sup>2</sup> | K(1E-6)<br>in-lb/rad | STATION DESCRIPTION |
|----------------------|----------|-----------------------------|----------------------|---------------------|
| .....                | 1        | 47.15                       | 1952.00              | MOTOR               |
| .....                | 2        | 94.29                       | 1952.00              | MOTOR               |
| .....                | 3        | 94.29                       | 1952.00              | MOTOR               |
| .....                | 4        | 94.29                       | 1952.00              | MOTOR               |
| .....                | 5        | 94.29                       | 1952.00              | MOTOR               |
| .....                | 6        | 94.29                       | 1952.00              | MOTOR               |
| .....                | 7        | 94.29                       | 1952.00              | MOTOR               |
| .....                | 8        | 94.29                       | 1952.00              | MOTOR               |
| .....                | 9        | 47.15                       | 102.70               | MOTOR               |
| .....                | 10       | 99.60                       | 11.69                | LS CPLG             |
| .....                | 11       | 64.20                       | 126.60               | LS CPLG             |
| .....                | 12       | 258.50                      | 289.40               | PINION              |
| .....                | 13       | 2.83                        | 30.00                | PINION              |
| .....                | 14       | 1.85                        | 139.60               | HS CPLG             |
| .....                | 15       | 1.85                        | 34.40                | COMPRESS            |
| .....                | 16       | 358.50                      | 0.00                 | COMPRESS            |

Figure 40. Mass/Elastic Data for Variable Frequency Motor System.

made to determine the cause of the failure. Analytical results predicted high stresses in the motor shaft for the first mode during startup (Figure 12). The torsional natural frequencies shown in Figure 41 are for full load (maximum coupling torsional stiffness) and are lower during startup. The first mode (17 Hz) can be excited by the 6th harmonic of electrical frequency at 60 rpm and by the fundamental electrical frequency at 800 rpm. A transient startup analysis predicted shaft stresses of 23,000 psi pk-pk at the low speed of 60 rpm; therefore, strain gages were considered to be the best method to measure the torsional response (both frequency and

EQUIVALENT SYSTEM MODE SHAPES

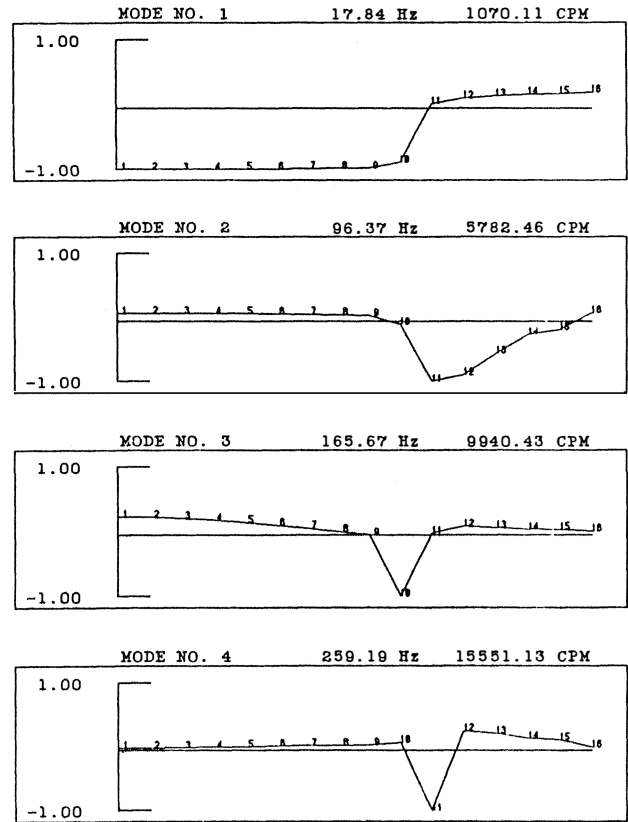


Figure 41. Natural Frequencies and Mode Shapes.

amplitude). Because of insufficient space for strain gages on the motor shaft, the strain gages were installed on the low speed gear shaft. The analytical model was used to convert the measurements to stress in the motor shaft. The measurements are shown in a time history format (Figures 42 and 43) and a speed raster format (Figure 44). Assuming a stress concentration factor of 3.0 at the keyway, the measured stress was 21,100 psi pk-pk. The measured

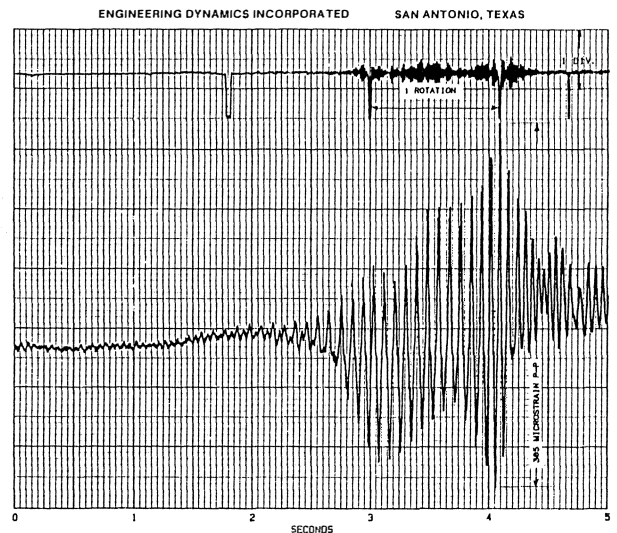


Figure 42. Strain Measurement on Gear Shaft At Initial Start.

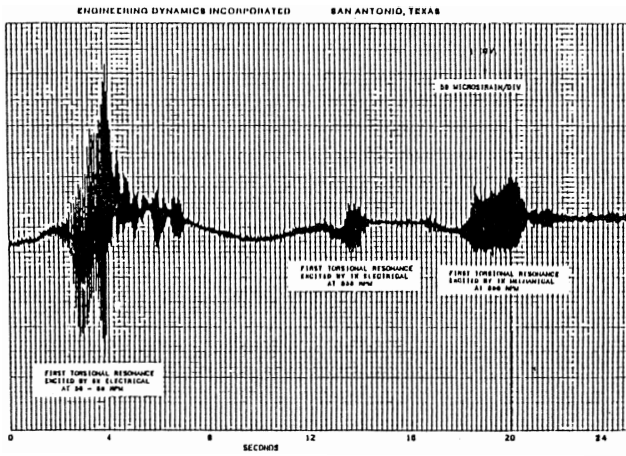


Figure 43. Strain Measurement on Gear Shaft During Runup.

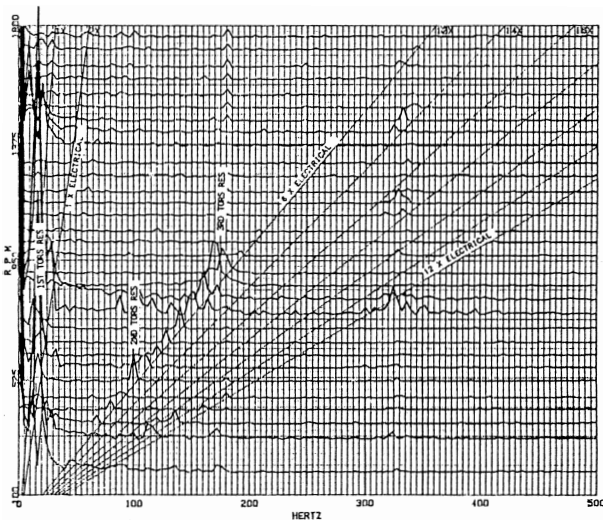


Figure 44. Speed Raster of Strain Measurements During Runup.

resonant frequencies of 17 Hz, 100 Hz, and 170 Hz compare to the calculated torsional natural frequencies of 18 Hz, 96 Hz, and 166 Hz.

**DEFINITION OF TERMS**

The *endurance limit* refers to the maximum stress level which would not cause a failure to occur even for an infinite number of stress cycles.

The *electrical frequency* is the fundamental exciting frequency providing the driving torque to a motor.

$$f_e = \frac{2f_m}{n} \tag{12}$$

where:  $f_e$  = electrical frequency, Hz  
 $f_m$  = rotational speed, rev/sec  
 $n$  = number of motor poles

The *full load rated torque* is the torque required to drive the system at rated speed for full load conditions.

*Mass-elastic properties* refers to the mass inertias ( $WR^2$ ) and the stiffnesses ( $K$ ) of the motor, fan, couplings and shafts. The natural torsional frequencies of the system are dependent upon these mass-elastic properties.

The *torsional natural frequency* is a frequency which requires minimal energy to respond to large amplitudes. It is determined by the mass-elastic properties of the shaft system. Critical speed and resonant frequency are equivalent terms.

*Peak-to-peak amplitude* is the difference between the instantaneous minimum amplitude and the subsequent maximum amplitude of the complex waveform. It is sometimes referred to as the double-amplitude.

*Steady-state* refers to an analysis for a system operating continuously at a speed. The analysis is repeated for each speed throughout the operating speed range.

*Transient* refers to a changing condition (startup or shutdown), a sudden load change or an electrical fault.

*Vibratory or dynamic torque* refers to the dynamic (modulating) component of torque in the coupling or in the shaft, which is a result of the response of the system to the input and load torques of the motor and fan.

*Zero-peak amplitude* is the difference between the average or equilibrium amplitude and the instantaneous maximum or minimum value of the complex waveform. It is sometimes referred to as the half-amplitude.

**APPENDIX**

*Holzer Method*

A common iteration method based upon equilibrium of torque at resonance can be effectively used to evaluate the natural frequencies and mode shapes of many shafting systems. The method originally used by Holzer was proposed as a tabular method designed for easy hand-calculations [3]. The main disadvantage of the procedure is the trial and error method of searching for the natural frequency which makes missing a frequency a possibility which can have serious ramifications.

The basis of the method is Newton's law translated into torsional terms:

|                      |                      |
|----------------------|----------------------|
| Linear Motion        | Torsional Motion     |
| $F = ma = m\ddot{x}$ | $T = J\ddot{\theta}$ |

for simple harmonic motion

$$\begin{aligned} \theta &= A \sin \omega t \\ \dot{\theta} &= A\omega \cos \omega t \\ \ddot{\theta} &= -A\omega^2 \sin \omega t = -\omega^2\theta \end{aligned}$$

For a shaft under free-vibration conditions (without a forcing torque;  $T = 0$ ),  $\sum J\omega^2\theta = 0$  will hold true only if  $\omega$  is the natural frequency. The values of the summation will be non-zero at nonresonant conditions; the non-zero value is called the residual torque. A plot of the residual torque versus frequency for a torsional system is shown in Figure A-1.

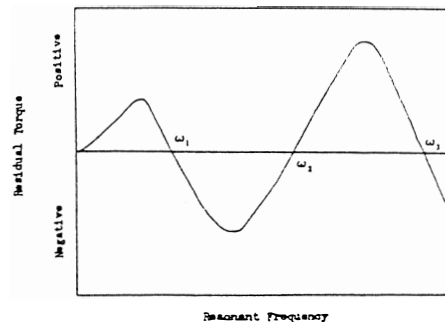
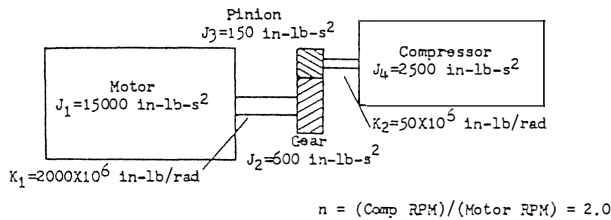


Figure A-1. Holzer Method Residual Torque.

Since the value of the summation is zero only at natural frequencies, it is obvious that the sign of the residual is opposite on either side of the natural frequency.

The Holzer method is begun by estimating (guessing) the first natural frequency and calculating the residual. An example torsional system given in Figure A-2 consists of a motor, gear and compressor. The Holzer calculations will be compared to the natural frequency calculated by the formulas in Blevins [5]. Using either the three mass equivalent system or the four mass geared system results in a frequency of 27.44 Hz (172.5 radians/sec).

ACTUAL SYSTEM



EQUIVALENT SYSTEM

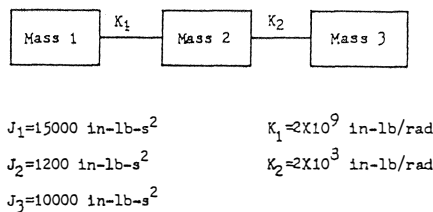


Figure A-2. Sample Torsional System.

To demonstrate the trial and error method, a value of 175 radians per second will be used as the first estimate for the Holzer tabulation.

Table A-1. Holzer Tabulation, First Iteration.

| $\omega = 175 \text{ rad/sec}$ |                         |          |                               |                                    |                 |   |
|--------------------------------|-------------------------|----------|-------------------------------|------------------------------------|-----------------|---|
| J                              | $J\omega^2 \times 10^6$ | $\theta$ | $J\omega^2\theta \times 10^6$ | $\sum J\omega^2\theta \times 10^6$ | $K \times 10^6$ | $\Delta\theta = \frac{\sum J\omega^2\theta}{K}$ |
| 15000                          | 459.375                 | 1.0      | 459.375                       | 459.375                            | 2000            | 0.2297  |
| 1200                           | 36.750                  | 0.7703   | 28.309                        | 487.683                            | 200             | 2.4384  |
| 10000                          | 306.250                 | -1.6681  | -510.857                      | -23.174                            |                 |   |

The residual torque value (-23.174) is negative. It indicates the estimate is above the natural frequency; reduce the estimate and recalculate.

Table A-2. Holzer Tabulation, Second Iteration.

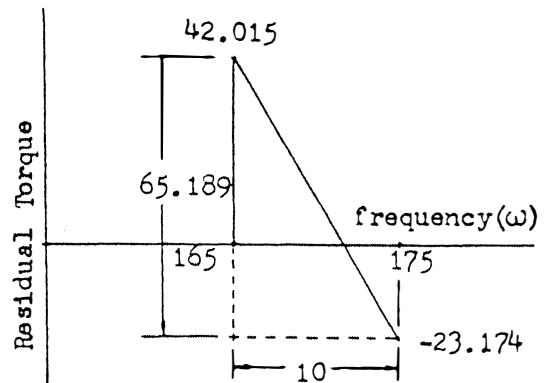
| $\omega = 165 \text{ rad/sec}$ |                         |          |                               |                                    |                 |   |
|--------------------------------|-------------------------|----------|-------------------------------|------------------------------------|-----------------|---|
| J                              | $J\omega^2 \times 10^6$ | $\theta$ | $J\omega^2\theta \times 10^6$ | $\sum J\omega^2\theta \times 10^6$ | $K \times 10^6$ | $\Delta\theta = \frac{\sum J\omega^2\theta}{K}$ |
| 15000                          | 408.375                 | 1.0      | 408.375                       | 408.375                            | 2000            | 0.2042  |
| 1200                           | 32.670                  | 0.7958   | 23.775                        | 432.150                            | 200             | 2.1607  |
| 10000                          | 272.25                  | -1.4330  | -390.135                      | 42.015                             |                 |   |

Because the residual torque (42.015) is positive, it is known to have gone below the natural frequency. Since it is known that the frequency is between 165 and 175 radians per second, a simple plot and proportionality of triangles can be used to determine a closer estimate of the natural frequency (Figure A-3).

Since the residual torque (+9.144) is a positive in the Holzer analysis, Table A3, the actual frequency is still higher. The answer after additional trials is 172.488 radians per second which compares closely to the closed-form solution.

Table A-3. Holzer Tabulation, Third Iteration.

| J     | $J\omega^2 \times 10^6$ | $\theta$ | $J\omega^2\theta \times 10^6$ | $\sum J\omega^2\theta \times 10^6$ | $K \times 10^6$ | $\Delta\theta = \frac{\sum J\omega^2\theta}{K}$ |
|-------|-------------------------|----------|-------------------------------|------------------------------------|-----------------|---|
| 15000 | 440.900                 | 1.0      | 440.900                       | 440.900                            | 2000            | 0.2204  |
| 1200  | 35.272                  | 0.7795   | 27.496                        | 468.397                            | 200             | 2.3419  |
| 10000 | 293.933                 | -1.5624  | -459.252                      | 9.144                              |                 |   |



$$\frac{10}{65.189} = \frac{x}{42.015} \quad x = 6.445$$

$$\omega \text{ for trial} = 165 + 6.445 = 171.445$$

$$\omega = 171.445 \quad \omega^2 = 29393.388$$

Figure A-3. Estimation of Next Guess for Holzer Method.

It is not necessary to get the residual torque to true zero, as long as the residual torque value is small in comparison to the torque values, which are in the millions. A reasonable target for the residual torque is 1000 (0.001 x 10<sup>6</sup>), which will provide sufficient accuracy for the natural frequency when the Holzer Table is completed. The column under theta represents the mode shape. In the example some values of theta exceed 1.0; therefore, to normalize the mode shape all values should be divided by the maximum value.

Table A-4. Comparison of Mode Shapes.

| $\theta$ | $\theta/1.5624$ | Actual Mode Shape |
|----------|-----------------|-------------------|
| 1.0      | 0.6400          | 0.6277            |
| 0.7795   | 0.4989          | 0.4876            |
| -1.5624  | -1.0            | -1.0              |

The third column is the mode shape based on the Holzer method for 172.488 radians per second.

## REFERENCES

1. Harris, C. M. and Crede, C. E., *Shock and Vibration Handbook*, Chapter 38, 2nd Ed., New York, New York: McGraw-Hill Book Co. (1976).
2. Nestorides, E. J., *A Handbook on Torsional Vibration*, British Internal Combustion Engine Research Association, pp.84-88 (1958).
3. Wilson, W. K., *Practical Solution of Torsional Vibration Problems, I*, New York, New York: John Wiley & Sons Inc. (1956).
4. Rotordynamics of Machinery, Engineering Dynamics Inc., Seminar, San Antonio, Texas (1991).
5. Blevins, R. D., *Formulas for Natural Frequency and Mode Shape*, Van Nostrand Reinhold Co. (1979).
6. Goldstein, H., *Classical Mechanics*, Addison-Wesley Publishing Co. (1965).
7. Szenasi, F. R., and VonNimitz, W. W., "Analyses of Synchronous Motor Trains," *Proceedings of the Seventh Turbomachinery Symposium*, Turbomachinery Laboratory, The Texas A&M University System, College Station, Texas (1978).
8. Wachel, J. C. and Sparks, C. R., "Pulsations in Centrifugal Pump and Piping Systems," *Hydrocarbon Processing*, pp. 183-189 (July 1977).
9. USAS B17.1-1967, "Keys and Keyseats," American Society of Mechanical Engineers (1973).
10. Peterson, R. E., *Stress Concentration Factors*, New York, New York: John Wiley and Sons (1974).
11. MIL STD 167-1 (SHIPS), Mechanical Vibrations of Shipboard Equipment (Reciprocating Machinery and Propulsion System and Shafting) Type III, IV and V (May 1974).
12. "Design Criteria and Alternate Analysis," Nuclear Power Piping, USAS B31.7-1969, ASME, Appendix F, p.167 (1969)
13. American Society of Metals, *Atlas of Fatigue Curves*, Editor H. E. Boyer, ASM (1986).
14. Shigley, J. E. and Mischke, C. R., *Mechanical Engineering Design*, 5th ed., New York, New York: McGraw Hill (1989).
15. Nishihara, M. and Fukui, Y., "Fatigue Properties of Full Scale Forged and Cast Steel Crankshafts," Conference on Component Design of Highly Pressure and Charged Diesel Engines, Institute of Marine Engineers (January 1978).
16. ASM Metals Reference Book, 2nd Ed., ASM (1982).
17. Dowling, N. E., "Fatigue Failure Predictions for Complicated Stress-Strain Histories," *Journal of Materials, JMLSA*, 7, (1), pp. 71-87 (March 1972).
18. Van Millingen, R. D. and Van Millingen, J. D., "Phase Shift Torquemeters for Gas Turbine Development and Monitoring," ASME paper 91-GT-189 (1991).
19. Verhoef, V. H., "Measuring Torsional Vibration," ISA Aerospace and Test Measurement Divisions Symposium, Las Vegas, Nevada (1977).
20. Rothberg, S. J. and Nalliwell, N. A., "On The Use of Laser Vibrometry for Rotating Machinery Measurements," *Proceedings of the Institution of Mechanical Engineers, Vibrations in Rotating Machinery* (1992).
21. Vance, J. M. and French, R. S., "Measurement of Torsional Vibration in Rotating Machinery," ASME paper 84-DET-55 (1984).
22. Perry, C. C. and Lissner, H. R., *The Strain Gage Primer*, New York, New York: McGraw-Hill Book Co., 2nd Ed. (1962).

## BIBLIOGRAPHY

- Rothbart, H. A., *Mechanical Design and Systems Handbook*, New York, New York: McGraw-Hill (1964).
- Szenasi, F. R. and Blodgett, L. E., "Isolation of Torsional Vibrations in Rotating Machinery," National Conference on Power Transmission (1975).
- Wachel, J. C. and Szenasi, F. R., "Field Verification of Lateral—Torsional Coupling Effects on Rotor Instabilities in Centrifugal Compressors," NASA CP2133 (1980).

